CHALMERS
UNIVERSITY OF TECHNOLOGY

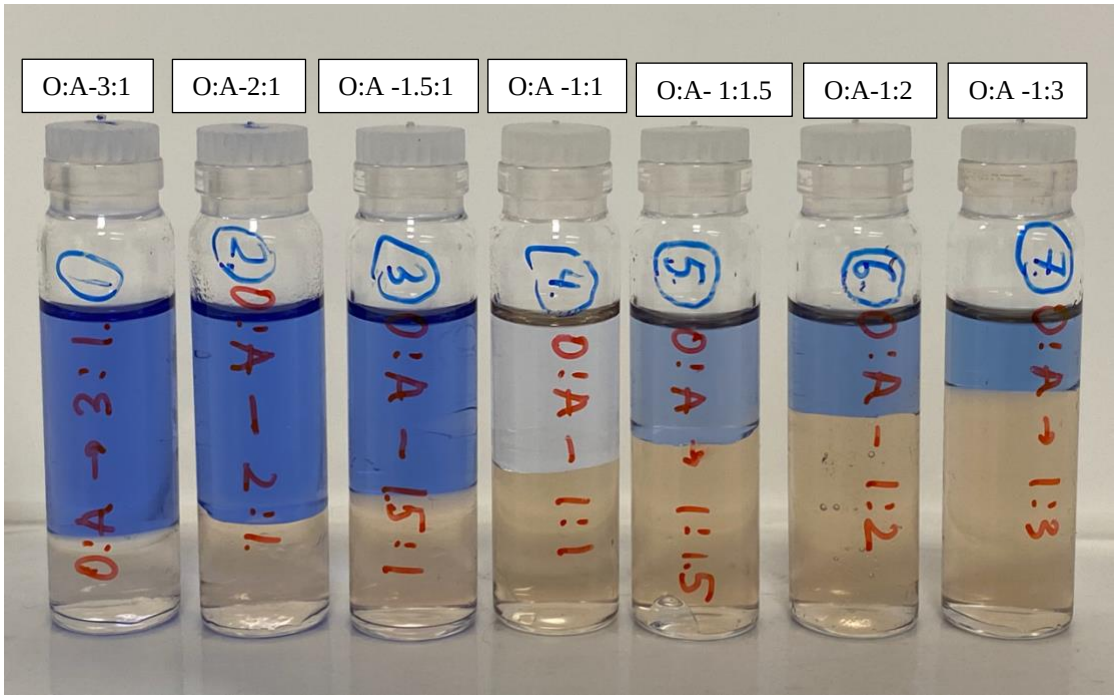

Recycling of spent lithium-ion batteries:

A study on the separation of manganese from cobalt, nickel and lithium in sulfuric media using solvent extraction.

Master's thesis in Innovative and Sustainable Chemical Engineering (MPISC)

AZIMOV SHERZOT

Department of Chemistry & Chemical Engineering
Chalmers University of Technology
Division of Energy and Materials
Gothenburg, Sweden 2022

Master's Thesis 2022

Recycling of spent lithium-ion batteries

A study on the separation of manganese from cobalt, nickel and lithium in sulfuric media using solvent extraction.

Azimov Sherzot

Supervisor: Dr.Nathália Cristine Vieceli, Chalmers University of Technology
Examiner: Dr. Martina Petranikova, Chalmers University of Technology

CHALMERS
UNIVERSITY OF TECHNOLOGY

Department of Chemistry & Chemical Engineering
Chalmers University of Technology
Division of Energy and Materials
Gothenburg, Sweden 2022
SE-412 96 Gothenburg
Telephone +46 31 772 1000

Recycling of spent lithium-ion batteries:
A study on the separation of manganese from cobalt, nickel and lithium in sulfuric media using solvent extraction.
AZIMOV SHERZOT

Supervisor: Dr.Nathália Cristine Vieceli, Chalmers University of Technology
Examiner: Dr. Martina Petranikova, Chalmers University of Technology

Master's Thesis 2022
Department of Chemistry & Chemical engineering
Chalmers University of Technology
Division of Energy and Materials
SE-412 96 Gothenburg
Telephone +46 31 772 1000

This research was supported by the Swedish Energy Agency – Battery Fund (Grants No: 40506-1 and 48204-1)

Cover: A set of vials used in the experiments to investigate the effect of the phase ratio on the extraction of Mn

Contents

List of Figures

List of Tables

Acknowledgments

First, I'd like to thank my examiner, Dr. Martina Petranikova, for the opportunity to write this fascinating thesis on the recycling of Li-ion batteries and introduce the important concept of recycling.
My supervisor, Nathália Cristine Vieceli, deserves credit for my master's thesis work: receiving excellent guidance for performing the experiments and writing this report. My master's thesis supervisor was exceptional, and I couldn't have asked for a better one.
Along with my supervisor and examiner, I would like to express my appreciation to Léa Rouquette for assisting me in comprehending the leaching mechanism. Thank you to Ioanna Teknetzi for her assistance with the ICP-OES analysis.
I also appreciate the recommendations provided by our Industrial Material Recycling and Nuclear Chemistry colleagues.
Last but not least, I'd like to express my gratitude to my family for their continuous encouragement.

This research was supported by the Swedish Energy Agency – Battery Fund (Grants No: 40506-1 and 48204-1)

Azimov Sherzot, Gothenburg, May 2022

Abstract

Manganese is an important alloying element that aids in the transformation of iron into steel. The steel industry consumes up to 90% of manganese globally, and it is expected that the expanding market for key non-metallurgical uses such as battery cathodes will have an increasing influence on its world market. Recycling in the steel and lithium-ion battery (LiB) sectors plays a critical role in meeting these needs. Solvent extraction for manganese recovery has been widely investigated to address this problem. However, there are drawbacks to this strategy, such as the co-extraction of metals and the infrequent consideration of the interplay of numerous factors that impact the metal extraction process. In this work, solvent extraction was utilized to improve manganese (Mn) extraction, reduce cobalt (Co) co-extraction, and eliminate high concentration contaminants like copper (Cu) and aluminum (Al) from spent (LiB) solution. Further, through the design of experiments and response surface methodology, it can be possible to identify and enhance influencing factors for manganese extraction by combining various variables. The best conditions for the extraction stage were found to be pH = 3.2, an O:A ratio of 1:1, and 0.5 M bis(2-Ethylhexyl) phosphoric acid (D2EHPA) with 15 minutes of contact time in this study. Mn extraction reached almost 89 % in a single extraction stage, with co-extraction of Co 2.5 %, which was then eliminated in two scrubbing stages. The optimal scrubbing stage operation conditions were discovered to be 6 g/L Mn (scrubbing solution – $MnSO_4.H_2O$), an O:A ratio of 1:1, and a contact time of 20 minutes. The ideal parameters for the stripping operation were determined to be 0.5 M sulfuric acid (H_2SO_4), an O:A ratio of 1:1, and a contact time of 15 minutes.

Keywords: solvent extraction, manganese, Li-ion batteries, D2EHPA, design of experiments

1. Introduction

Manganese (Mn) is in great demand due to its usage in the manufacturing of steel and batteries (i.e., cathode material). Manganese is a common metal with an atomic number of 25 that is equally as important as iron (Fe) in the production of contemporary industrial societies' fundamental building blocks. It is the 12th most prevalent element, accounting for around 0.1% of the Earth's crust. Mn is a critical and irreplaceable component of steelmaking, and just a few countries control the worldwide mining sector. In addition, the United States includes Mn as one of the most critical minerals [1].

When iron ore is turned into iron, manganese eliminates oxygen and sulfur. Manganese can also be found in alloys with metals like aluminum and copper. As an alloy, it makes steel less brittle and gives it more strength[1].

Although manganese ores are found all over the world, the majority of the supply comes from a small number of mining zones. In 2011, just four nations produced 70% of the world's manganese ore: South Africa, Australia, China, and Gabon. 90% of proven manganese reserves are also in these four countries, plus Brazil and Ukraine. [1] For this reason, the United States and Europe have long been concerned about manganese ore supply in the event of political or military interruptions in production or supply networks [1].

In the electric vehicle (EV) sector, lithium-ion batteries (LiBs) are widely utilized. In the long run, LiBs chemistry development is becoming increasingly significant, and nickel-manganese-cobalt oxide (NMC) cathode materials that contain more lithium and manganese than existing versions, could presumably boost energy density and safety while cutting prices. However, a trade-off must be made to improve one or two features. In this scenario, raising the manganese and lithium levels lowers the cathode's stability, causing it to operate differently over time[2]. A manganese-rich cathode battery, however, is becoming the star of the show, slightly overtaking nickel (Ni), which is less costly and safer than one with high nickel content [3].

Manganese metal has a high electronegativity, which means it has low reactivity and is thus safe to handle in water [4], [5]. It also has a low reduction potential of 1.19 V vs. standard hydrogen electrode (SHE) and a large capacity of *7250 mAh cm^{-3}* and *976 mAh g^{-1}* when two electrons are exchanged[6]. Manganese's qualities make it an obvious option as an anode material in high-voltage aqueous batteries, and the amount of manganese in the cathode material has a significant influence on the battery cells' safety, which is a top consideration when it comes to batteries that power electric automobiles and electronics [7].

In 2020, the overall LiBs market was estimated to be worth USD 40.5 billion. The market is expected to grow at a compound annual growth rate (CAGR) of 14.6% from now until 2026 when it will be worth nearly USD 92 billion [8]. *Figure 1a* depicts the global battery consumption, which is predicted to rise from 185 GWh in 2020 to more than 2,000 GWh by 2030, which, is mostly attributable to the electrification of transportation [9]. Specifically, *Figure 1b* shows that

under the Sustainable Development Scenario (SDS**) vs. IEA's Stated Policies Scenario (STEPS*), global manganese demand is expected to expand dramatically by 2040, reaching about 8 times the demand volume in 2020 [10].

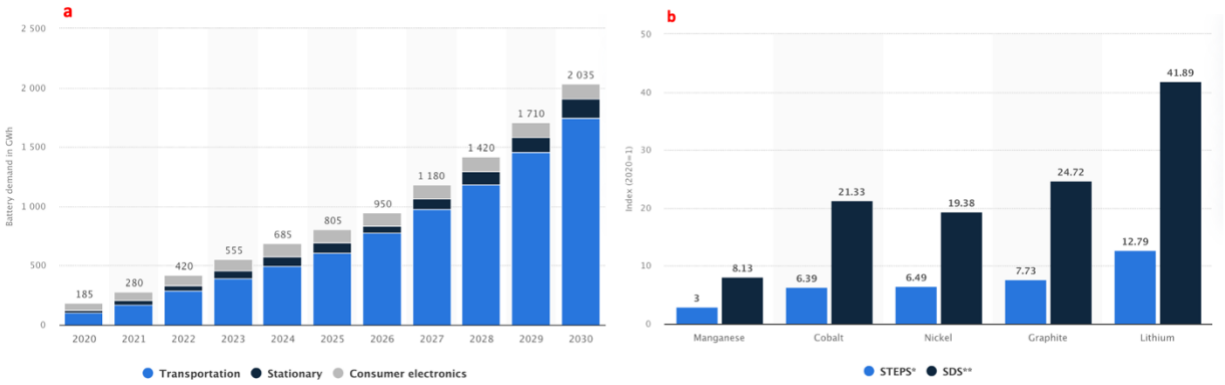

Figure 1a. Global battery demand forecasts from 2020 to 2030, broken down by application (in gigawatt hours) (1b). Demand growth index for selected battery-related minerals in clean energy technologies throughout the world in 2040 compared to 2020, per scenario [9][10]

As more industries required resources, the depletion of certain metals and minerals expanded, but recovery methods began to improve in efficiency as the industry became more technologically advanced. In this context, there have been a substantial number of studies on recycling LiB waste, but most of them have centered on the recovery of Li, Co, and Ni, with Mn recovery being less extensively explored [11], [12]. The present technologies for recovering Mn from primary resources are inappropriate for recovering Mn from LiBs waste, which, together with the relatively low price of Mn (e.g., US$1860-2060 per metric ton, 2018 year), diminishes the momentum for better Mn recovery procedures [12], [13]. In addition, when it comes to recycling LiB waste, Mn is seen as a problematic contaminant. The presence of Mn in LiBs waste has been demonstrated to impact the quality and efficiency of cobalt (Co) alloy manufacturing [14].

There have been several research publications on Mn extraction using solvent extraction. However, there has been little study on the topic of linking factors that affect extraction. According to a study carried out by Xuan et al. (2022), the critical variables that influence Mn metal extraction are contact time, an O:A ratio, pH equilibrium, D2EHPA extractant concentration, and temperature [15].

2. Theory

2.1 Main constituent elements in batteries

Lithium-ion batteries (LiBs) are becoming widely attractive due to their affordability and practicality. As shown in *Figure 2*, LiBs typically include four main components: cathode, anode, electrolyte, and separator [16]. The weight percentage of the main components of the most recent LiBs is depicted in *Figure 3.* The anode and cathode combined account for the most weight in LiBs, accounting for 40%, the current collectors for 15%, the electrolyte for 11%, and the separator has a 4% weight. Other components, such as the casing and tab, account for 30% of the total weight [17].

Li metal oxides or phosphates, such as $LiMn_2O_4$ (Lithium Manganese Oxide, LMO) and $LiFePO_4$ (LFP), are frequently used as cathodes in LiBs, whereas graphite materials are used as anodes. The choice of anode and cathode materials is critical, and this is where many researchers are concentrating their efforts. The microporous layer (separator) made of polypropylene (PP), polyethylene (PE), and other types of polymers is used to isolate the positive and negative regions and reduce battery short-circuiting between the two poles. The electrolytes (e.g., lithium salt ($LiPF_6$) in organic solution) that transfer lithium ions between the anode and cathode electrodes play a critical role in maximizing the performance of LiBs, such as improving battery cycle life, lithium-ion transmission, and safety properties. Furthermore, the electrolyte design, as well as the amount of additives used, are significant [18].

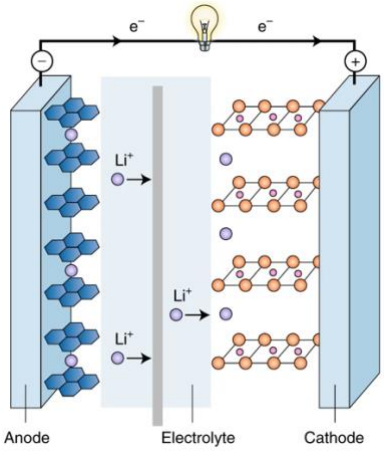

Figure 2. Main components of a rechargeable Li-ion battery (LiBs.[16].

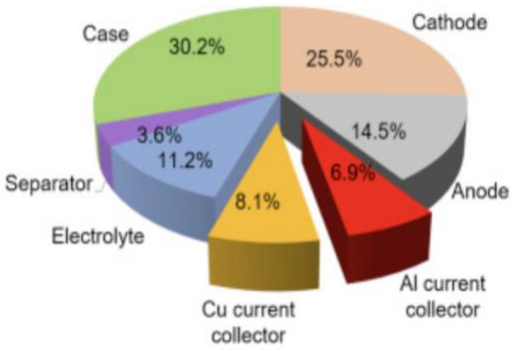

Figure 3. The weight percentage of main components in LIBs[17].

During the charge/discharge state, Li ions can flow between the cathode and the anode via the electrolyte, as shown in *Figure 4* [18]. When discharging, electrons flow from the anode to the cathode electrode, whereas Li-ions pass through the electrolyte. An external electrical power source forces electrons and Li-ions to move in the opposite direction during the charging state [19].

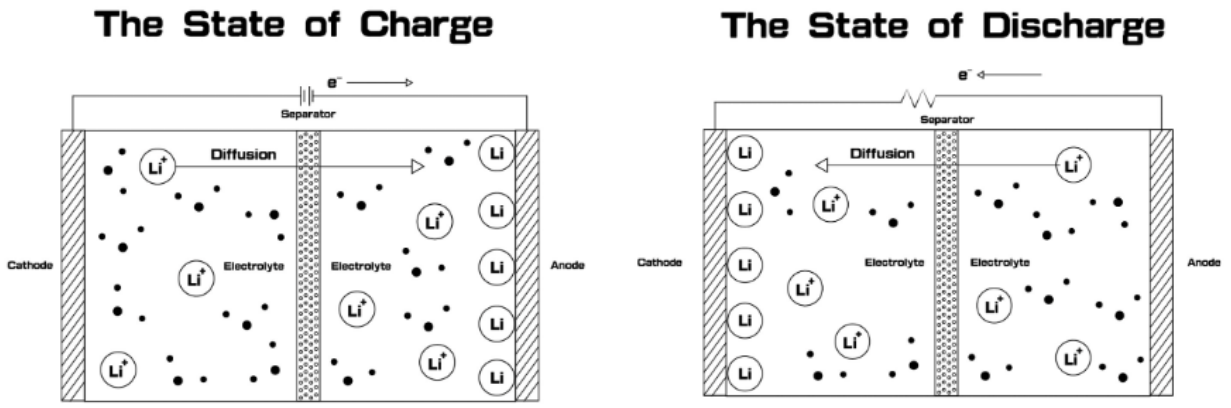

Figure 4. Discharge/charge operations are depicted schematically in a lithium-ion battery (LiBs)[18].

2.2 Processes for recycling spent Li-ion batteries

Lithium-ion battery recycling is commonly divided into three types of recycling methodologies: mechanical, pyrometallurgical, and hydrometallurgical. Moreover, various strategies can be utilized in conjunction with one another[20]. Mechanical processing entails discharging, crushing, and separating the battery components using mechanical technologies such as magnetic, and gravimetric separation. Hydrometallurgical procedures comprise the extraction of components from batteries via dissolving, depending on the acid solubility of the components contained in the active organic or inorganic materials [21]. Besides, there is high-temperature processing, in which metal recovery from pyrometallurgical processes involves reducing component metal oxides to an alloy of Cu, Fe, and Ni in a high-temperature furnace [22].

2.2.1 Pretreatment steps

The pretreatment process is critical in Li-ion recycling. Since it improves the recovery factor while also lowering electricity usage. Pretreatment's main purpose is to safely and effectively segregate the various elements that makeup LiBs. Discharge, dismantling, separation, dissolution, and thermal treatment are examples of pretreatment processes [23].

2.2.1.1 Discharging of spent LiBs

To minimize short-circuits and flames once the battery packs are not drained, which could trigger the burning of volatile organic compounds, and flammable solvents during the dismantling process. Therefore, used unit cells normally undergo a discharging stage before mechanical disassembly. In addition, water electrolysis produces a significantly slower discharge rate, and the discharge rate may be greatly enhanced by including solution ions in the discharge step [24].

2.2.1.2 Dismantling

Unlike portable unit cells, which may be destroyed without any special treatment, automobile batteries must be dismantled manually. However, most unit cell disassembly is done

mechanically with the use of crushers. Based on Kim et al. (2021) study, during the disassembly of the spent LiBs, the release of volatile flammable solvents was explored. (i.e., dimethyl carbonate, and tert-amylbenzene). Therefore, all important safety issues must be addressed when disassembling battery packs [23], [25].

2.2.1.3 Mechanical pretreatment spent LiBs

Mechanical processing of disassembled LiBs is required to fragment batteries, segregate specific components, and concentrate the black matter to free the active materials. This is a critical stage for hydrometallurgical processing. Magnetic separation, crushing, sieving, and classification are the primary processes that are utilized during the mechanical pretreatment of discarded LiBs. The purpose of these procedures is to obtain a fraction that is richer in cathode active material (black mass). After being subjected to crushing and distribution, the separator, aluminum foils, copper foils, and plastics are found to make up the majority of the coarse aggregates, whilst the electrode materials, such as Lithium Cobalt Oxide (LCO) and graphite, are found in the fine fraction. During the magnetic separation process, the different magnetic properties of the different types of steel are taken into account [26].

2.2.1.4 Thermal treatment and pyrometallurgy

Thermal treatment is primarily used to remove organic molecules and graphite from electroactive materials and concentrate them into powder. Organic chemicals such as polyvinylidene fluoride (PVDF) are utilized as binders and pose issues in leaching and phase separation. In most cases, the thermal treatment is conducted as incineration (in the presence of oxygen) or as pyrolysis (in the absence of oxygen) [27]. In the pyrometallurgical processing, critical elements are reduced and subsequently reclaimed in the form of alloys. This has numerous advantages, including simpler scaling and the use of fewer chemicals. However, pyrometallurgical operations have in general lower reprocessing effectiveness than hydrometallurgical processing, and one of the disadvantages is that Li will end up in the slag [28] [29].

2.2.2 Hydrometallurgical process

Unlike pyrometallurgical treatment, hydrometallurgy usually allows for the recovery of lithium. The hydrometallurgical recycling process may be divided into four parts: leaching, impurity removal, metal recovery (Mn, Ni, Co), and lithium recovery. More specifically, after being slurried with mild acid, the wasted cathode material is delivered to the leaching chambers. The leaching chambers are subsequently filled with acid and under reducing conditions, extract Mn, Ni, Co, Fe, Al, and Li. Undesired contaminants can be eliminated by pH adjustment in the impurity elimination stage. The solution is then transported to the material recovery section, where the metal can be extracted using solvent extraction or precipitation. The residual lithium-enriched solutions are passed to the lithium extraction area after metal recovery, where lithium can be extracted through chemical precipitation using sodium carbonate (Na_2CO_3) or crystallization.

Figure 7 shows the general flowsheet of combined mechanical and thermal pretreatment with the hydrometallurgical process for the recycling of LiBs [30].

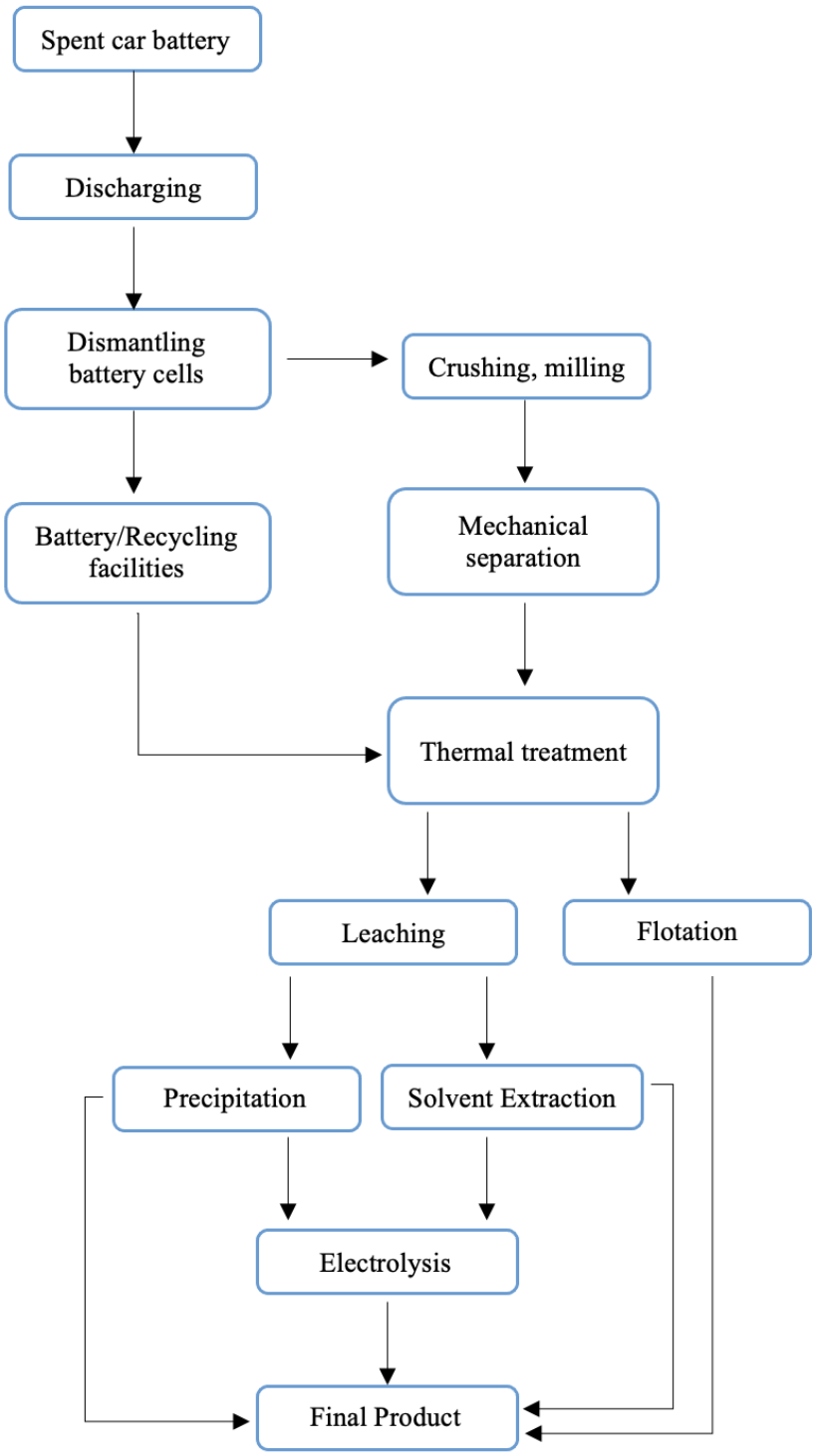

Figure 5. General flow sheet of the combined treatments starting from LiBs waste until reaching the final product. Adapted from [27].

2.2.2.1 Leaching

The leaching solution commonly comprises inorganic acids, including sulphuric acid (H_2SO_4), nitric acid (HNO_3), aqua regia (NHO_3+3HCI), or hydrochloric acid (HCl). Mainly, the leaching effectiveness of spent LiBs is influenced by the concentrations and composition of the leaching solution, such as pH equilibrium, liquid to solid ratio, and temperature. Additionally, organic reducing agents may be utilized in the leaching step. [31] One of the various reducing agents used in leaching is sodium bisulfite ($NaHSO_3$), hydrogen peroxide (H_2O_2), and certain polysaccharides, such as ascorbic acid ($C_6H_8O_6$), are introduced to enhance the leaching of metallic ions through converting the insoluble metal ions Mn^{4+} to soluble Mn^{2+} in the aqueous medium. For instance, with the addition of reductants such as H_2O_2 and ascorbic acid to the leaching solution, cobalt leaching efficiency may reach 99% [32].

2.2.2.2 Precipitation

Precipitation has been used to extract impurity metal ions from leachates. It offers a straightforward procedure and a reasonably high rate of recovery of metals from spent LiBs. Before solvent extraction of Ni and Co, contaminants such as Fe, Cu, and Al are normally removed from the leachate by precipitation with sodium hydroxide (NaOH). After removal of Co, Ni and Li can also be recovered by precipitation using Na_2CO_3 [27].

2.2.2.3 Solvent Extraction

Solvent extraction is a popular method for separation because of its convenience, efficiency, and versatility. Solvent extraction is often quite selective, and the separation of the desired component may typically be accomplished by repeating the extraction operation multiple times. Solvent extraction is essential in the purification of various chemical industries such as mining, LiBs recycling, semiconductors, and nuclear fields [33].

Certain solvent extraction methods for high-value metals have become economically feasible and have been developed, and metal recovery by liquid-liquid separation is also frequently used as a technique in chemical analysis for sample preparation [33]. Several organic extractants, such as D2EHPA, Cyanex 272, and PC-88A, have been employed in solvent extraction to segregate and collect metal ions [27].

2.2.2.3.1 Bis(2-Ethylhexyl) phosphoric acid(D2EHPA)

The structure of Bis(2-Ethylhexyl) phosphoric acid (D2EHPA) is depicted in *Figure 6.* Due to its chemical consistency and great selection, Bis(2-Ethylhexyl) phosphoric acid has been considered to be a useful extractant in hydrothermal procedures for the isolation and identification of a variety of different metals. Additionally, it is available commercially, is affordable, and is well-known for Co^{2+} and Mn^{2+} metal ion extraction. The sequence of primary metal extraction in LiBs by D2EHPA is Mn > Co > Ni. [34] In the nuclear field, D2EHPA is the most investigated extractant, and it is considered a more effective extractant than Versatic acid ($C_{10}H_{20}O_2$), being able to recover heavy lanthanides even at low pH [33].

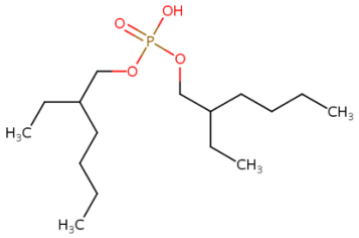

Figure 6. The structure of Bis(2-Ethylhexyl) phosphoric acid (D2EHPA)[35].

2.2.2.3.2 $C_{16}H_{34}PO_2H$ (Cyanex 272) and (PC-88A)

The most effective extractant for extracting Co^{2+}over Ni^{2+} is Bis(2,4,4-trimethylpentyl) phosphinic acid (Cyanex272). Cyanex 272 is an acidic extractant that has a strong preference for Co^{2+} over Ni^{2+} in sulfate and chloride environments, which attracts a large number of researchers. The Cyanex 272 has a large separation factor of >1000 (Co: Ni ratio of 1000:1), and the separation efficiency of Ni^{2+} and Co^{2+} is increased when the equilibrium pH of the actual solution is increased. The main advantages of Cyanex 272 are that it is easy to handle and that it is also non-toxic. However, when compared to other extractants, the cost of Cyanex 272 is significant. In addition, Cyanex 272 and its salts (e.g., ammonium and sodium) were proven to be highly successful and specific for the isolation of metallic elements from leaching fluid solutions, including Ni^{2+}, Co^{2+}, Cu^{2+}, Zn^{2+} and Fe^{2+} sulfates formed from raw nickel sulfate [36].

The (2-ethylhexyl phosphonic acid mono-2-ethylhexyl ester) PC-88A is a selective extractant for recovering Nickel and Lithium from cathode scrap sulfate leachate. It has advantages due to its ease of handling and high purity of final nickel product (99%) [37]. According to Ahn et al. (2012), the extraction % of Ni and Li, as well as the separation factor of Ni/Li, increased as the equilibrium pH was increased using PC-88A [38].

3. Scope of Work

The main goal of this work is to examine and optimize the separation of manganese from leachate resulting from the acid leaching of black mass from spent LiBs using solvent extraction. In this master thesis work, the solvent extraction process will be studied, which is part of the hydrometallurgical process to recover spent LiBs, employing Bis(2-Ethylhexyl) phosphoric acid (D2EHPA) as the primary extractant agent, ($MnSO_4.H_2O$) as the scrubbing solution in the scrubbing operation and sulphuric acid (H_2SO_4) in the stripping operation.

First, a preliminary range of solvent extraction parameters was determined to separate Mn using D2EHPA as the extractant. Then, using a design of experiments (DoEs), the solvent extraction of Mn was optimized. The final step was to investigate optimal conditions for the scrubbing and stripping operations.

4. Aim and Objective

Global stocks of discarded batteries have grown as a result of the dramatic increase in demand for Li-ion batteries (LiBs). The hydrometallurgical process is an innovative recycling method that is both environmentally friendly and effective at recovering valuable metals. To make the process economically feasible, the process parameters should be tuned. This study's purpose and goals are as follows:

- Investigate and optimize the separation of manganese from leachate obtained by the acid leaching of black mass from spent LiBs using solvent extraction.
- Determine a preliminary range of conditions for the solvent extraction of Mn using D2EHPA as an extractant.
- Optimize the solvent extraction of Mn using design of experiments (DoEs) and McCabe-Thiele diagrams.
- Investigate the effect of the main process variables (pH, organic to aqueous ratio, the concentration of extractant, and contact time) on the recovery of Mn from the leachate.
- Examine the impact of key process variables on scrubbing and stripping operations.

5. Materials and Methods

The general process flowsheet of performed experiments comprising extraction, scrubbing, and stripping is depicted in *Figure 7*. First, the extraction process transfers the target metallic ions from the aqueous feed solution to the organic phase (loaded organic). After the extraction stage, the scrubbing operation removes undesired co-extracted metal ions from the loaded organic phase, using a solution containing the target metal (e.g., $MnSO_4.H_2O$). After removing the co-extracted metal ions from the loaded organic, stripping is employed to remove the Mn metal ion into the aqueous phase. It can be done using a stripping solution like H_2SO_4 to revert the extraction reaction.

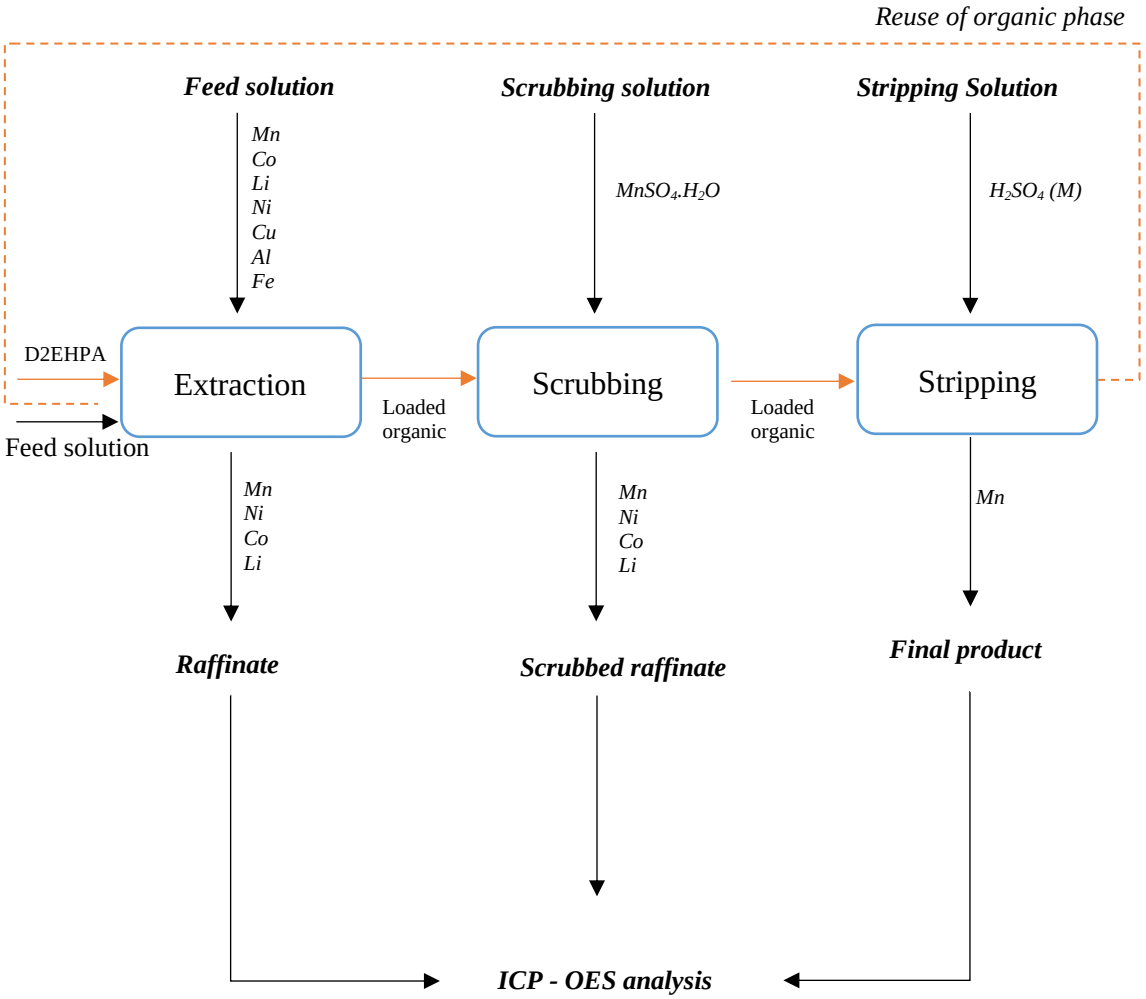

Figure 7. General process flowsheet of extraction, scrubbing, and stripping of performed experiments. Orange lines represent the organic phase and black the aqueous phase.

The procedure for preparing the leachate solution is as follows. The leachate was generated via acid leaching of spent LiBs using 2 M H_2SO_4 and 3% H_2O_2 (59% w/w), an S/L ratio of 1:20 g/ml at 50 ^{0}C for 60 min in a single large reactor and experiment (no replicates). After leaching, the pH of the leachate was increased to 5.1 using 10 M NaOH aiming at removing some of the main impurities (Cu, Al, Fe) to produce the final solution to be used in the solvent extraction tests (feed solution). As a solvent extraction reagent, D2EHPA (Bis(2-Ethylhexyl) phosphoric acid, 97%, Sigma Aldrich) was used. The diluent was Isopar L (Exxon Mobil).

All the experiments were conducted at room temperature. The preliminary extraction tests were conducted in a shaking machine (IKA- Vibrax) set to 1000 vibrations per minute, using glass vials of 3.5 ml, and a contact time of 15 min was selected based on a literature review [39], [40] to ensure the excellent phase contact. The effect of some process conditions (O:A ratios, concentration of extractant) on the extraction efficiency was evaluated and all preliminary test conditions will be presented in the result and discussion section.

After selecting the conditions for Mn extraction based on the preliminary experiments, the operation was optimized using the factorial design of experiments and response surfaces. For the design of experiments, the extraction tests were performed using plastic containers of 50 ml with a mechanical stirrer from mixer-settlers coupled on their top. All the tests were performed at room temperature with a stirring speed of 1000 rotations per minute. The experimental conditions used in the design of experiments are presented in *Section 5.3*.

The pH of the aqueous phase was determined using a pH meter (Metrohm827 pH lab), which was regularly calibrated before and during the experiments. The 3.2 pH (optimal condition) was adjusted using 10 M NaOH based on preliminary results. After 15 minutes of contact time at the appropriate pH, samples from the aqueous were taken for analysis. When a lack of clear phase separation was observed, the samples were centrifuged (Ohaus^R, 5000 rpm for 5 min)

After determining the optimal conditions for extraction, a larger volume of loaded organic was obtained under those conditions to be used in the scrubbing tests. Then, the scrubbed loaded organic solution based on the optimal scrubbing conditions for the stripping tests was prepared.

Chemical analysis of samples was performed using Inductively Coupled Plasma – Optical Emission Spectroscopy from the aqueous phase (ICP-OES, iCAP^{TM} PRO**).** The samples for ICP-OES analysis were diluted with HNO_3 (0.5 M containing 1 ppm Y). Yttrium was used to monitor the analysis and the concentrations of each metal in the aqueous solution. Different standards were used (20, 10, 5, 2.5, 1.25, 0.625 ppm) for the determination of the relationship between intensity (wavelength) and concentration using ICP-OES. The standards encompass several different metals usually encountered in Li-ion battery chemistry (Fe, Na, Li, Al, Cu, Co, Mn, Ca, Zn, P, and Mg)

Aqueous and organic phases make up the leachate solution. The concentration of the feed solution is known, and a mass balance is used to quantify the residual concentrations in the feed solution after extraction. The concentration [M^+] *org. out* is determined from the mass balance in *Equation 1*.

$$[M^+]_{aq,in} * V_{aq,in} + [M^+]_{org,in} * V_{org,in} = [M^+]_{aq,out} * V_{aq,out} + [M^+]_{org,out} * V_{org,out} \quad \text{Equation 1}$$

In and *out* represent flows entering and leaving the system respectively, *org* is an organic phase, *aq* is the aqueous phase, *v* is volume, and [M^+] is the concentration of the ion metal under concern.

Equation 2 was used to estimate the metal extraction efficiency:

$$(\%)E = 100 * \frac{V_{feed.sol(aq)} - V_{conc.sample(aq)}}{V_{feed.sol(aq)}} \qquad \textit{Equation 2}$$

$V_{feed.sol(aq)}$ is the concentration of the feed solution in the aqueous phase, whereas $V_{conc.sample\ (aq)}$ is residual concentrations in the feed solution after extraction.

Where:

Using *Equation 3*, the distribution ratio (D) can be found by dividing the concentration of a solute in the organic phase ($C_{organic}$) by its concentration in the aqueous phase ($C_{aqueous}$). This shows how well the species are extracted

$$D = \frac{C_{organic}}{C_{aqueous}} \qquad \textit{Equation 3}$$

5.1 Setup of Factorial Design of Experiments

Factorial designs of experiments are an effective way of obtaining an empirical mathematical model that links the response variable with factors, often called independent variables. Thus, the factorial design of experiments was used to explore and simulate the impact of significant design factors. The methodology is explained in detail by Montgomery (2013)[41]

A full (2^k) factorial design of experiments was utilized to estimate linear main effects and identify significant 2^{nd}order effects of the linear regression model. The full factorial plane can be represented as 2^k, obtaining $n=2^k$ as the series of experiments (n). To determine the response (y), three variables (k=3) with two levels each were evaluated (2^3-factorial design). In addition, four more experiments were conducted at the factor center level to verify the experimental error, and the axial points were geometrically situated in the middle of the faces of a cube ($\alpha = 1$).

The variables addressed in the design of experiments to represent the extraction stage are pH (x_1), an organic to aqueous ratio O:A (x_2), and the molar concentration of D2EHPA M (x_3). All the experiments were run in random order, and the conditions of each test can be observed in *Table 3* (*Section 6.1.3*). The factors addressed in the factorial design of experiments for the extraction stage are presented in *Table 1*.

Table 1. Variables and correspondent levels were used in the design of experiments of the extraction stage.

Variables	***Unit***	***Levels***		
		High (+1)	***Standard (0)***	***Low (-1)***
Equilibrium pH, (x_1)	dimensionless	4	3.2	2.4
Organic to the aqueous phase, O:A (x_2)	dimensionless	2	1.5	0.5
Concentration of D2EHPA (x_3)	M	0.5	0.4	0.3

The linear least-square method was used to fit the parameters of a linear 2nd-order regression model to the experimental results. Only significant variables were included in the models (p-values smaller than the significance level of 95%, 0.05). In addition, an ANOVA was performed to test the estimated model's validity.

The coefficient of Determination (R^2) was used to represent how well an estimated regression calculation describes the variance of the response variable. In addition, response surfaces and contour plots were used to explore more optimal variations and points, which will be shown in the results and discussion *(Section 6.1.4*).

6. Results and Discussion

6.1 Preliminary experiments of Extraction

The starting pH of the feed solution (leachate) was 4.8, and its initial elemental composition can be seen in *Table 2.*

Table 2. Elemental composition of the leachate (feed solution) obtained by acid leaching of black mass followed by precipitation.

Metal	***Leachate concentration (mg/L)***
Co	2666
Mn	2055
Ni	2429
Cu	1340
Li	908
Al	340
Fe	10.2
Mg	3.6
Zn	2.35

The best range of conditions for future inquiry using a factorial design of experiments was identified in preliminary studies. The extraction of Mn using D2HEPA as the extractant is identified in the literature as a fast process. For instance, the extraction of metals such as Mn, Ni, Co, and Li has been described in the literature when varying contact durations by Chen et al. (2014). At first, Mn extraction was around 60% after 5 minutes of contact time and increased to 70% after 10 minutes using an O:A ratio - 1:1, 0.5 M D2EHPA, and an equilibrium pH of 3.5. The maximal level of Mn extraction was obtained after 15 minutes (~75%) and remained stable for the next 15-60 minutes. Besides, after 5 minutes of contact time, co-extraction of Co, Ni, and Li increases somewhat but stays less than 15%. After 10 minutes, the increase in Mn extraction resulted in almost constant co-extraction of the other metals. Consequently, the co-extraction of Li, Ni, and Co was around 3%, %, 5%, and 11.5%, respectively.[39] Thus, according to Chen et al. [39] and Hossain et al. [40]], the thermodynamics of Mn extraction using Co-D2EHPA have been observed to be fast. Based on this information from the literature, the contact time was fixed at 15 minutes in this study.

6.1.1 Effect of the different concentrations of D2EHPA and equilibrium pH

The extraction of Mn, Co, Li, and Ni for four distinct molar concentrations of D2HEPA (0.3, 0.4, 0.5, and 0.6 M) at various equilibrium pH levels are shown in *Figure 8(a-d)*

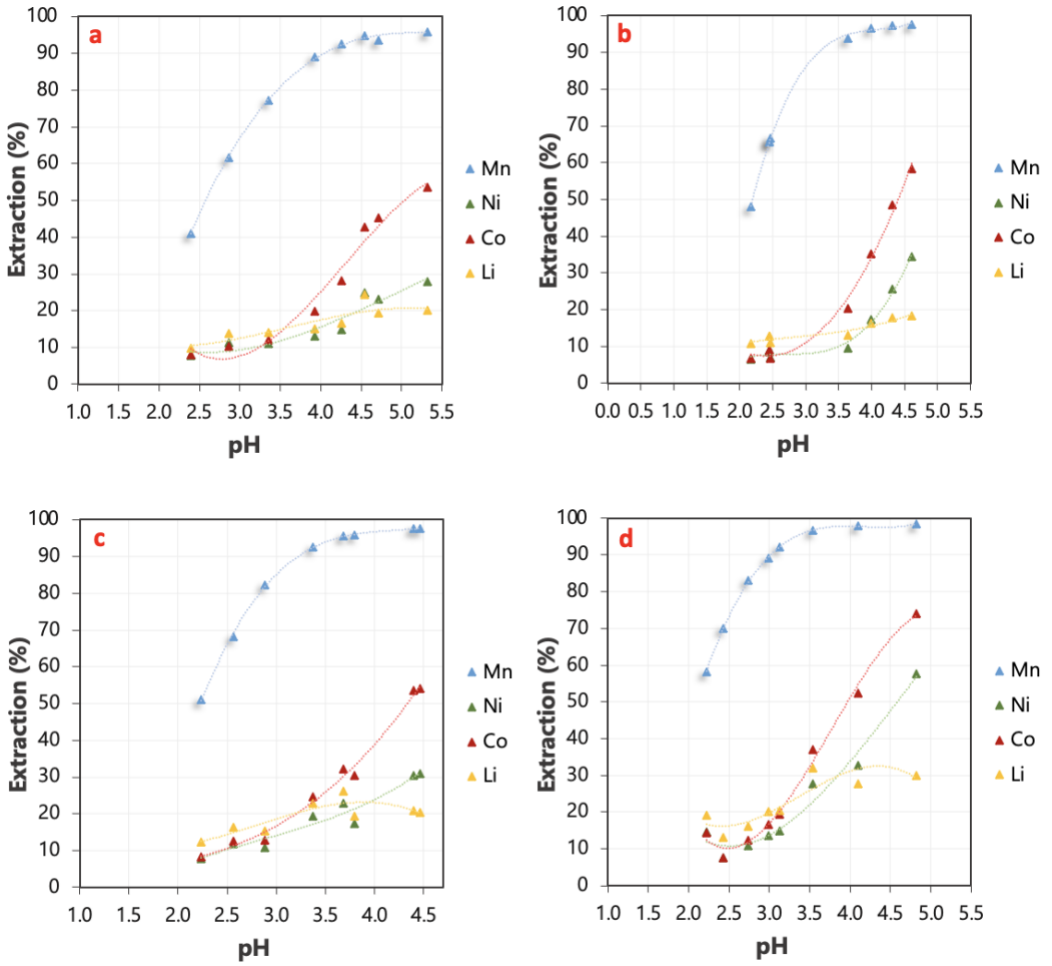

Figure 8. Different molar concentrations of D2EHPA were used to extract metals: (a) 0.3 M D2EHPA, (b) 0.4 M D2EHPA, (c) 0.5 M D2EHPA, and (d) 0.6 M D2EHPA, and O:A of 1:1 (ml) with a 15 min contact time.

In *Figure 8(a-d)* the extraction of Mn increased as the molar concentration of D2HEPA increased, which was more obvious when 0.6 M D2EHPA was utilized. For the four distinct concentrations of D2EHPA, the manganese extraction increased with pH, but as the pH was increased to around 3.5, co-extraction of other metals, mainly Co, became more evident. High co-extraction of other metals should be minimized and one of the primary objectives of these preliminary tests was to find the range of conditions that allows achieving the lowest co-extraction of Co while achieving the highest extraction efficiency for Mn, for further optimization using factorial design of experiments. Thus, the ideal pH range will be between 3.1 and 3.2.

After interaction with the D2EHPA extractant, the pH of the aqueous phase was decreased to a range of 2.1 and 2.2 (from 4.8). This is explained by the metal extraction phenomena caused by D2EHPA. In *Equation 4* outlined by Zhang and Cheng [42], which results in a decrease in pH while the metal-organic complex releases the hydrogen protons, this outcome is predicted.

$$M^{2+} + 2(\overline{HA})_2 \overset{reaction}{\Longleftrightarrow} \overline{MA_4H_2} + 2H^+ \qquad \text{Equation 4}$$

Where M^{2+} stands for metal, $\overline{(HA)}_2$ is D2EHPA in the organic phase, and $\overline{MA_4H_2}$ stands for the metal-organic complex.

The co-extraction of minor impurity metals Cu, Mg, Zn, and Al from the leachate is presented in *Figure 9(a-d)* using the same concentrations of D2EHPA 0.3, 0.4, 0.5, and 0.6 M and varying the equilibrium pH levels. Except for Zn, all graphs *in Figure 9(a-d)* depict the same trend for the Cu, Mg, and Al – their co-extraction grows exponentially as pH rises. This is particularly evident for Cu and Al and when the pH is over 3.5, their coextraction exceeds 80% and 50 %, respectively. The co-extraction of Zn is nearly constant regardless of the pH value. Therefore, except for Zn, it is possible to conclude that the extraction efficiency of all main metals investigated increases with pH, under the tested conditions.

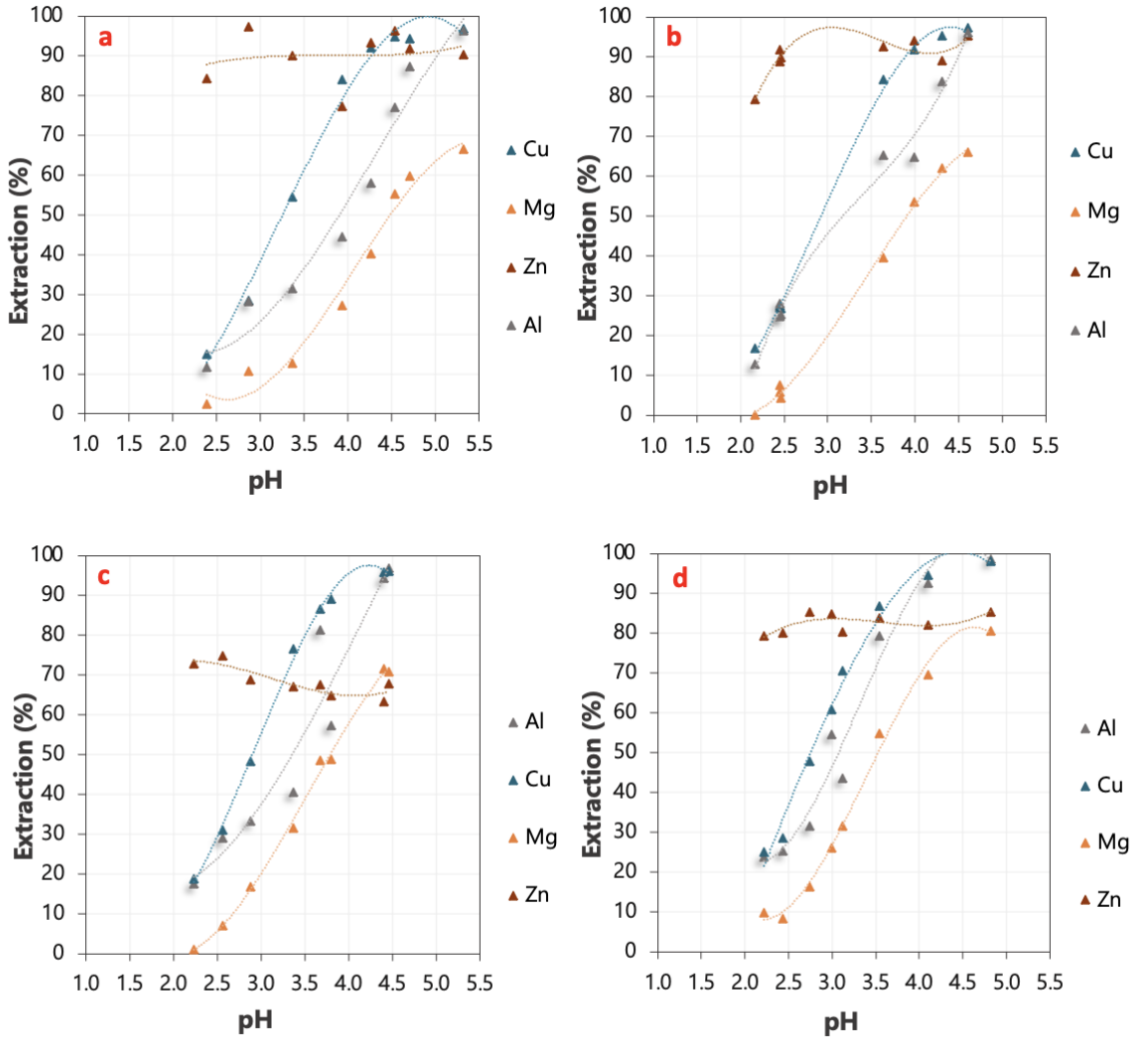

Figure 9. Effect of pH and different concentrations of D2EHPA on the co-extraction of metals Al, Cu, Mg and Zn (a) 0.3 M D2EHPA, (b) 0.4 M D2EHPA, (c) 0.5 M D2EHPA, and (d) 0.6 M D2EHPA, and an O:A of 1:1 with a 15 min contact time.

For example, the extraction of all major metals (Mn, Co, Li, Ni, Al, Cu, Mg, and Zn) from the leachate solution using 0.4 M D2EHPA is depicted in *Figure 10*. It is showing Logarithmic Distribution Ratio (Log D) where it is clear that pH findings have a significant impact on all metal extractions.

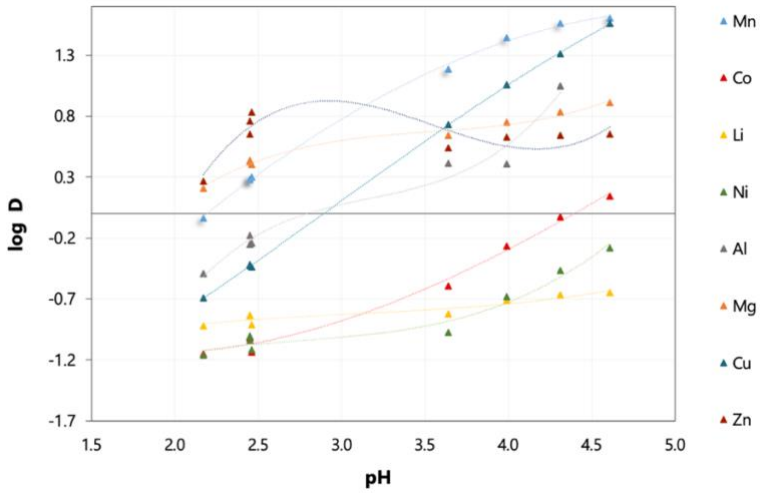

Figure 10. Logarithmic Distribution Ratio (Log D) of 0.4 M D2EHPA to extract the metals. Conditions: O:A of 1:1 (3ml) with a 15-minute contact time.

However, it can be seen that a high co-extraction efficiency of Al and Cu is simultaneously in *Figure 10*. In addition, those metals (e.g., Co, Cu, and Al) are present in high concentrations in leachate solutions which are shown in *Table 2*. Therefore, it is possible that these impurity metals may be present in the final product containing Mn. Thus, additional techniques must be developed to remove these metals from the leachate in order to reduce their concentration in the final product (e.g., precipitation or cementation should be done before starting to extract the main metals such as Mn, Co, Ni, and Li).

Considering the primary purpose of the preliminary tests as depicted in *Figure 9(a-d)*, which compared extractant concentrations of 0.3, 0.4, 0.5, and 0.6 M, it is most appropriate to continue further experiments using 0.4 M D2EHPA and 3.2 equilibrium pH. Since under these conditions, it is possible to reach high extraction efficiency for Mn, use less concentration of extractant while keeping co-extraction of other metals at low levels.

6.1.2 Effect of the Organic to Aqueous Ratio (O:A)

Preliminary studies were carried out to see how the Organic to Aqueous (O:A) ratio affected metal extraction. The tests were performed using the following O:A ratios 3:1, 2:1, 1.5:1, 1:1 and the main results can be observed in *Figure 11(a-b)*. It is possible to observe that the extraction of Mn increased along with the O:A ratio, however, the co-extraction of Co also

increased. For instance, while Mn extraction surpassed 95% with an O:A ratio of 1.5:1, the co-extraction of Co, Cu, and Al under the same conditions was 32 %, 80%, and 50 %, respectively.

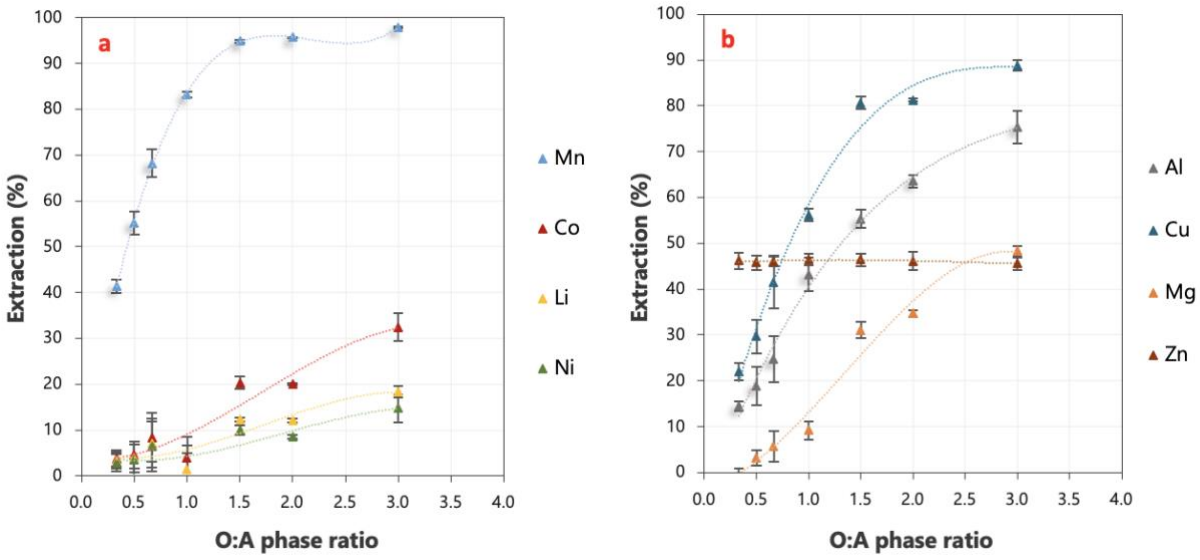

Figure 11 (a-b). Effect of different O:A ratios and 0.4 M D2EHPA on the extraction of metals with a 15-min contact time. The standard deviation of triplicates is represented by the error bars.

A similar tendency can be seen in *Figure 11b* as the O:A ratio rises so does the amount of metal co-extraction of minor impurities. (e.g., Al, Cu, and Mg). The ratio of Al to Cu in the leachate solution is not particularly high to compare Co and Mn. However, a substantial amount can still affect the final product. Besides, the equilibrium pH and O:A ratio variation did not influence Zn metal extraction, which remained constant under the tested conditions. However, it is important to highlight that the concentration of Zn and Mg in the leachate is much lower than the other metals, as presented in *Table 3.* The error bars depict the standard deviation of triplicates.

The McCabe-Thiele diagrams can be used to estimate the number of countercurrent stages necessary for Mn metal extraction methods. The distribution of Mn in the organic and aqueous phases may be observed in *Figure 12*. The operational line represents the phase ratio for an O:A. This line indicates that an increase in the metal concentration in the organic phase is equal to a decrease in the metal concentration in the aqueous phase multiplied by the phase ratio. Therefore, complete extraction of Mn could be possible after two extraction stages with an O:A ratio of 1:1. The error bars depict the standard deviation of triplicates.

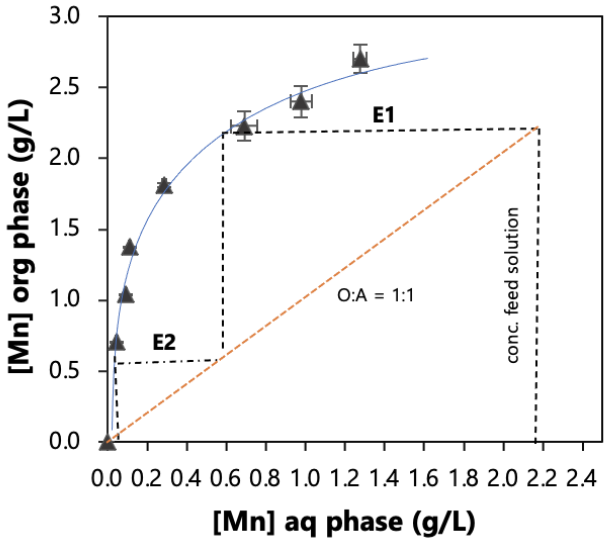

Figure 12. McCabe-Thiele diagram of the Mn extraction using an O:A ratio - 1:1. The concentration of Mn in the feed solution is 2177 mg/L. Conditions: pH of 3.2, 0.4 M D2EHPA and contact time of 15 min.

6.1.3 Setup of Factorial design of experiments and regression model.

The conditions used in the factorial design of experiments and the correspondent extraction efficiencies as a response are shown in *Table 3* for different metals.

Table 3. Conditions used in the factorial design of experiments (real variables) and respective responses as extraction efficiency of different metals (Mn, Ni, Li, Co, Al, Cu, Zn). All experiments were conducted in random order.

Random order	Standard order	Coded variables			Real Variables			Y (Extraction)						
		x1	x2	x3	pH	O:A	D2EHPA	Mn(%)	Co(%)	Li(%)	Ni(%)	Al (%)	Cu(%)	Zn (%)
6	1	-1	-1	-1	2.4	0.5	0.3	10.7	0.0	0.0	0.00	49.2	0.0	72.0
11	2	1	-1	-1	4	0.5	0.3	51.1	0.0	0.0	0.00	92.5	49.4	87.9
17	3	-1	1	-1	2.4	2	0.3	50.6	0.0	0.0	0.00	58.6	9.6	86.2
10	4	1	1	-1	4	2	0.3	97.1	32.4	4.8	8.13	99.2	92.3	87.8
9	5	-1	-1	1	2.4	0.5	0.5	28.7	0.0	0.0	0.00	53.6	2.7	81.2
12	6	1	-1	1	4	0.5	0.5	79.7	1.4	0.0	0.00	98.8	73.9	88.3
13	7	-1	1	1	2.4	2	0.5	74.0	0.0	2.1	0.00	68.9	26.5	86.7
2	8	1	1	1	4	2	0.5	99.0	64.2	20.4	41.17	98.7	96.1	88.0
3	9	0	0	0	3.2	1	0.4	79.3	2.1	0.8	0.00	93.7	46.4	88.0
4	10	0	0	0	3.2	1	0.4	80.2	2.1	0.5	0.00	88.7	48.1	88.2
14	11	0	0	0	3.2	1	0.4	79.0	0.3	1.1	0.00	87.4	46.3	88.5
8	12	0	0	0	3.2	1	0.4	79.7	1.4	1.0	0.00	92.2	46.9	88.4
7	13	-1	0	0	2.4	1	0.4	38.0	0.0	0.0	0.00	59.6	2.6	83.1
1	14	1	0	0	4	1	0.4	91.7	17.0	2.1	3.47	85.8	84.8	88.2
18	15	0	-1	0	3.2	0.5	0.4	49.0	0.0	0.0	0.00	77.0	20.7	86.5
15	16	0	1	0	3.2	2	0.4	94.7	11.8	7.6	2.40	95.1	75.7	88.2
16	17	0	0	-1	3.2	1	0.3	65.7	0.0	0.0	0.00	88.3	31.9	87.6
5	18	0	0	1	3.2	1	0.5	88.1	2.6	0.0	0.00	94.2	60.9	87.3

All experiments were conducted in random order and at room temperature with a contact time of 15 minutes. Experiments 1–8 are sequentially related to the baseline of 2^3 factorial design (standard order). The replicates at the design's center point (experiments 9–12) were used to estimate the experimental error, which was chosen based on the optimal conditions. Experiments 13-18 integrate axial points into the structure.

The Analysis of variance (ANOVA) of fitted models Mn, Li, Co, Cu, and Al are shown in *Table 4.* The methodology is explained in detail by Montgomery (2013)[41]

Table 4. ANOVA of the fitted models for the extraction of Mn, Co, Li, Cu, and Al with assessing experimental error and dividing the Residual into Pure Error and Lack of Fit.

Response source		Degree of freedom	Sum of squares	Mean square	F	Significance F
Manganese (Mn)	Regression	10	10747.0	1074.7	63.4	6.6E-06
	Residual	7	118.7	17.0		
	Lack of fit	*4*	*117.8*	*29.4*	*98.0*	*1.6E-03*
	Pure error	*3*	*0.9*	*0.3*		
	Totals	17	10865.6			
Cobalt (Co)	Regression	10	4503.3	450.3	33.1	6.0E-05
	Residual	7	95.2	13.6		
	Lack of fit	*4*	*93.0*	*23.3*	*32.3*	*8.4E-03*
	Pure error	*3*	*2.2*	*0.7*		
	Totals	17	4598.5			
Lithium (Li)	Regression	10	403.5	40.4	20.6	2.90E-04
	Residual	7	13.7	2.0		
	Lack of fit	*4*	*13.5*	*3.4*	*60.2*	*3.39E-03*
	Pure error	*3*	*0.2*	*0.1*		
	Totals	17	417.2			
Cupper(Cu)	Regression	10	15900.1	1590.0	19.7	3.36E-04
	Residual	7	564.3	80.6		
	Lack of fit	4	562.4	140.6	225.6	4.76E-04
	Pure error	3	1.9	0.6		
	Total	17	16464.4			
Aluminum(Al)	Regression	10	4613.6	461.4	19.1	3.71E-04
	Residual	7	168.7	24.1		
	Lack of fit	4	142.5	35.6	4.1	1.39E-01
	Pure error	3	26.2	8.7		
	Total	17	4782.3			

The core level of the design's replicates enables for assessment of experimental error and dividing of the Residual into Pure Error and Lack of Fit. The results of the F-test reveal the importance of the fitted models. When compared to the residual error, the experimental error at the center point of the design is low, and the variance of the experimental error is modest. In addition, for every metal (Mn, Co, Li, Cu, Al) lack of fit is not significant.

Since Mn, Co, Li, Cu, and Al are present in high initial quantities in leachate, they are considered to be major metals of concern. The regression models for those metals on their extraction efficiencies are depicted in *Equations 5-9*, respectively.

These models are valid only within the design range (for the parameters evaluated in this work) and only variables with a significant effect on responses were included in the models ($\alpha = 0.05$)

$$Mn(\%) = 78.24 + 21.66x_1 + 19.62x_2 + 9.42x_3 - 12.09x_1^2 - 4.04x_1x_2x_3 \qquad \textit{Equation 5}$$

$$Co(\%) = 1.58 + 11.5x_1 + 10.7x_2 + 3.57x_3 + 11.9x_1x_2 + 4.14x_1x_3 + 3.79x_2x_3 + 3.79x_1x_2x_3 + 6.85x_1^2 \quad \textit{Equation 6}$$

$$Li(\%) = 0.79 + 2.51x_1 + 3.48x_2 + 1.77x_3 + 2.88x_1x_2 + 1.69x_1x_3 + 2.21x_2x_3 + 1.69x_1x_2x_3 + 3.05x_2^2 \quad \textit{Equation 7}$$

$$Cu(\%) = 47.05 + 35.51x_1 + 15.34x_2 + 7.71x_3 \quad \textit{Equation 8}$$

$$Al(\%) = 88.9 + 18.5x_1 + 4.95x_2 - 14.57x_1^2 \quad \textit{Equation 9}$$

Pareto charts of the standardized effects of the factors on the responses are shown in *Figure 13(a-e)*. The standardized effects are the t-statistic results obtained by regression analysis. The t-static is calculated by dividing the coefficients by the standard errors.

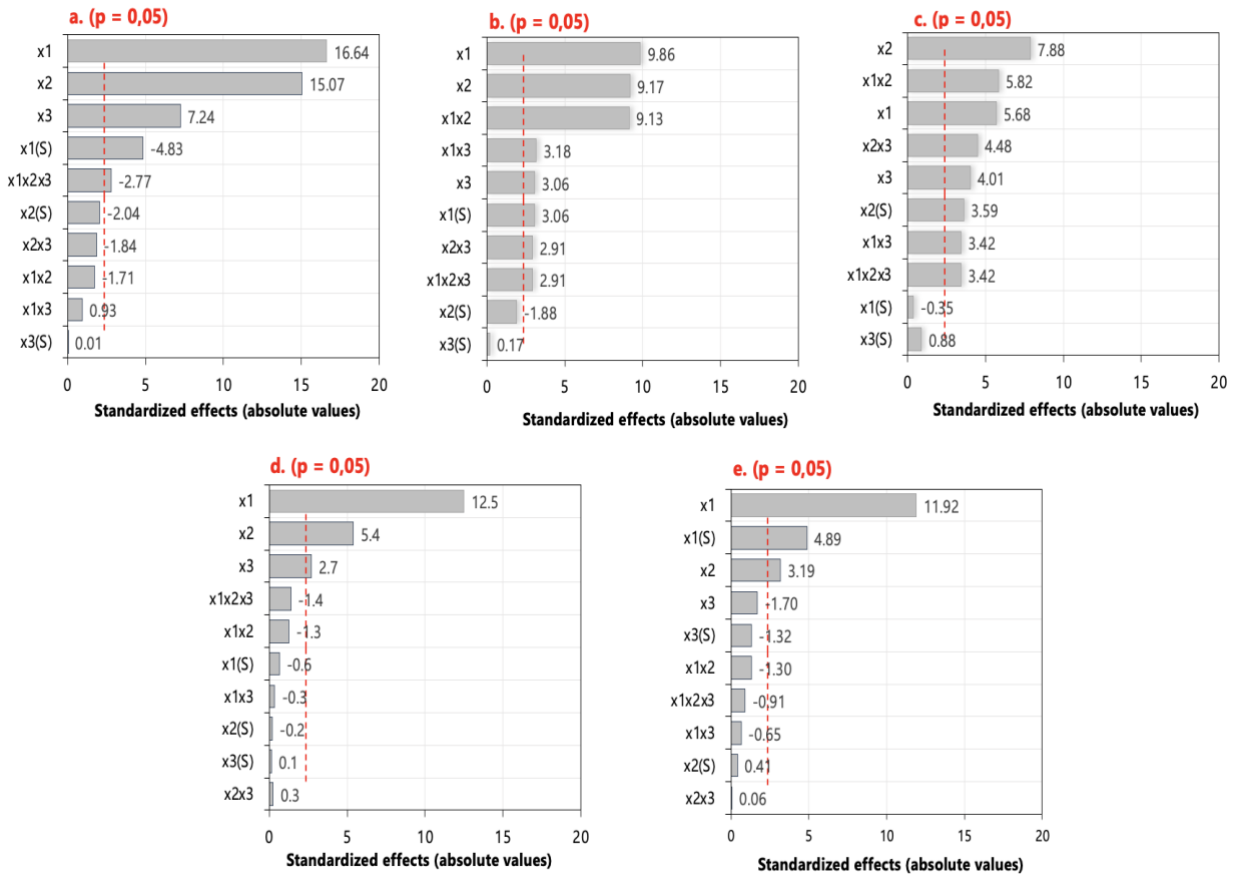

Figure 13(a-e). Pareto charts showing the standardized effects of the factors for the regression model for (a). Mn, (b). Co, (c). Li,(d). Cu and (e). Al. (S): square, x_1: pH, x_2: O:A ratio, and x_3: D2EHPA. The confidence level of 95%.

Dashed lines (2.36 at abscissa) indicate the significance level in the plots. The most important variables are those above the red dashed line, and those parameters are used in the regression model presented above. The most important parameters affecting manganese extraction

were x_1: pH, x_2: an O:A ratio, and x_3: molar concentration of D2EHPA. The x_1(square) and interaction of all three parameters ($x_1x_2x_3$) are also significant in the extraction of Mn, as shown in *Figure 13a.* It can be demonstrated that when the pH, O:A ratio, and molar concentration of D2EHPA increase, manganese extraction increases as well.

The most important parameters that accounted for the Co co-extraction were x_1: pH, x_2:an O:A ratio, and x_1x_2: interaction of pH and O:A ratio, as shown in *Figure 13b,* from highest to lowest in terms of significance (95%). Besides, x_1x_3, x_3, x_1(S), x_2x_3, $x_1x_2x_3$, and x_2(S) interactions are also significant but at a lower scale (all of them above dashed line).

The most significant variables responsible for Li co-extraction were x_2: O:A ratios, x_1x_2: interaction between pH and O:A ratio, and x_1: pH with the largest influence in terms of confidence level (95%), as shown in *Figure 13c.* x_3, x_2(S), x_1x_3, x_2x_3 , and $x_1x_2x_3$ are also major interactions, but at a lower scale.

The most critical factors impacting the co-extraction of Cu were x_1: pH, x_2: (O:A) ratio, and x_3: molar concentration of D2EHPA, as shown in *Figure 13d.* Thus, Cu co-extraction rises with increasing pH, O:A ratio, and molar concentration of D2EHPA. Same as Mn extraction efficiency behavior.

The key impacting factors accounted for in the Al co-extraction as shown in *Figure 13e* are x_1: pH, x_1(S): pH, and x_2: O:A ratio, in terms of confidence level (95%). The remaining parameters are all located under the dashed line (not significant). Therefore, it can be concluded that Al co-extraction increases as pH and the O:A ratio increase.

The coefficient of determination (R^2) was used to evaluate the models' accuracy. The scatter plots in *Figure 14* show how the experimentally observed and model-predicted responses are related.

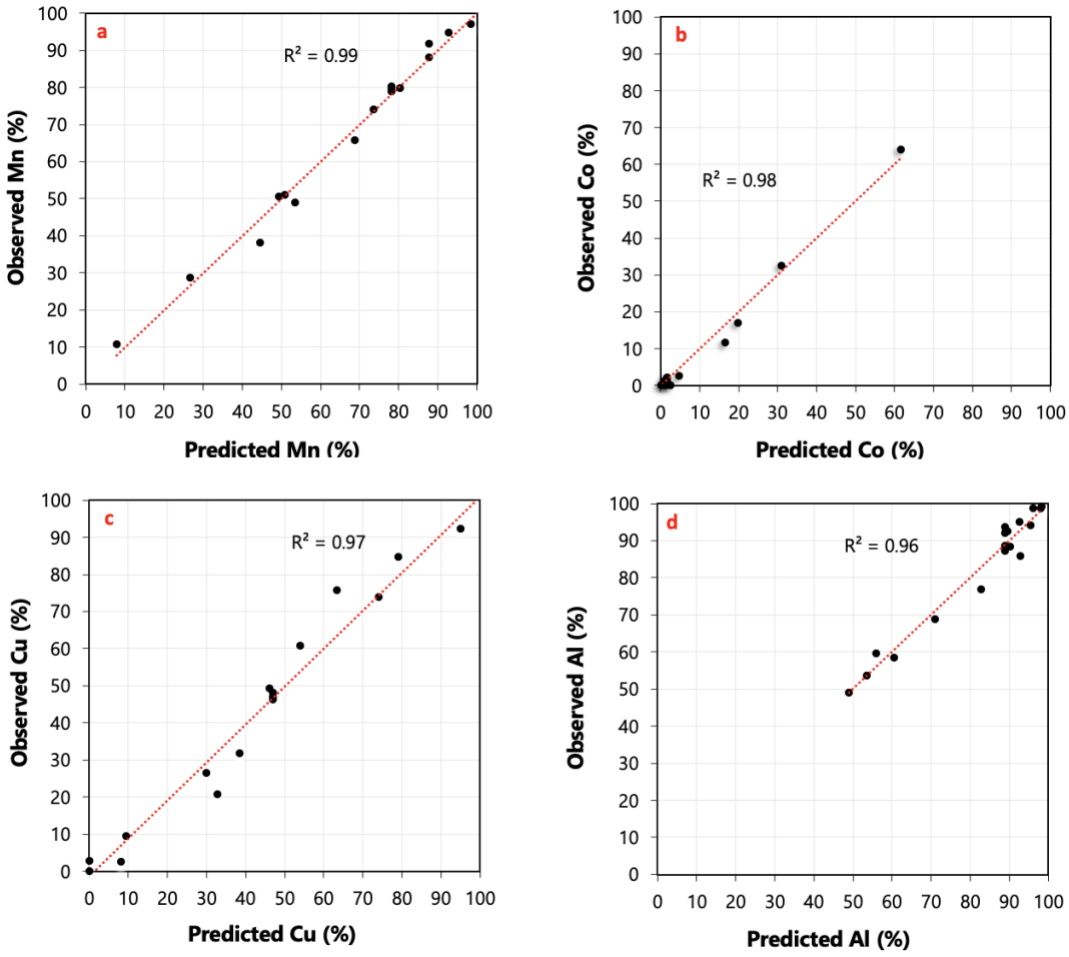

Figure 14. Experimentally observed vs predicted (%) by the model. (a). Mn, (b). Co, (c). Cu, and (*d).* Al *extraction.*

The coefficients observed in *Figure 14* imply that the 99%, 98%, 97%, 97%, and 96% of the response variability for Mn, Co, Cu, and Al, respectively, can be explained by the fitted models. This relationship shows that the fitted models are capable of providing a good fit to the observed results. Additionally, within the range of values studied in this research, the highest extraction efficiency for Co is 62%, while the lowest extraction efficiency for Al is 45%. The co-extraction of Li never exceeded 20% and this metal was omitted from the scatter plots.

6.1.4 Response Surfaces: Extraction of Mn, Co, Cu, and Al

Different factors have been utilized in the extraction of the primary metals, and the response surface is the simplest approach to display the association between them. Response surfaces help to analyze a procedure in which factors impact the response of concern, to optimize the output. The contour plot is created by combining a collection of responses with a pair of variables. In this study, the impact of pH is directly related to the molar concentration of the extractant D2EHPA and the organic to aqueous O:A ratios. Varying the levels of O:A ratios and

concentration of D2EHPA resulted in the construction of contour plots for each metal using the extraction efficiency as the response and setting the pH as constant in its low level 2.5, standard level 3.2, and high level 4 as depicted in *Figure 15(a-l).*

When x_1(pH) is set at the highest level (+1=4) the greatest extraction of Mn (99%) is obtained, while the concentration of D2EHPA is 0.5 M and the O:A ratio is 2:1, as can be seen in *Figure 15a.* When x_1 was adjusted to the standard level (0=3.2) the lower Mn extraction (50%) was obtained when the concentration of D2EHPA was 0.3 M and the O:A ratio was 0.5:1 *(Figure 15b).* The lowest extraction of Mn (11%) was found when the x_1 was set to the lowest level (-1=2.4) and the concentration of D2EHPA was 0.3M and the O:A ratio was 1:2 in *Figure 15c.*

A similar trend was observed for the co-extraction of Co. When the x_1: (pH) is adjusted to the high level (+1=4), the greatest co-extraction of Co is achieved 57% when the concentration of D2EHPA is 0.5 M, and the O:A ratio is 2:1, as can be seen in *Figure 15d.* When the pH was adjusted to the standard level (0=3.2), the maximum co-extraction of Co 20% was achieved for 0.5 M D2EHPA, and the O:A ratio is 2:1. When the x_1: (pH) was set to the lowest value (-1= 2.4), the co-extraction of Co did not exceed 2.5-5 % under any conditions. Thus, it is possible to conclude that under the tested conditions, the co-extraction of Co grows only in the presence of high concentrations of D2EHPA or O:A ratios.

Cu and Mn had similar behavior. When the x_1 (pH) is set to the high level (+1= 4) the maximum co-extraction of Cu 99% is attained while the concentration of D2EHPA was 0.5 M and the O:A ratio was 2:1 as shown in *Figure 15g*. The lowest co-extraction of Cu ∼59% was achieved when the concentration of D2EHPA was 0.3 M and the O:A ratio was 1:2. When x_1 is set to the standard level (0= 3.2) the higher co-extraction of Cu 70% is observed when the concentration of D2EHPA is 0.5 M and the O: A ratio is 2:1in *Figure 14h,* while the smallest co-extraction ∼24% occurs when the concentration of D2EHPA is 0.3 M and the O:A ratio is 1:2. Finally, when the x_1(pH) was adjusted to the lowest level (-1=2.4), the maximum co-extraction of Cu achieved was in the range of 35% when using 0.5 M D2EHPA and an O:A ratio of 2:1. The lowest effectiveness of co-extraction of Cu ∼ 2% was found when the concentration of D2EHPA was set at 0.3 M and the O:A ratio was 1:2.

When x_1 (pH) is adjusted to the high level (+1= 4) the greatest co-extraction efficiency of Al 97% was achieved with a D2EHPA concentration of 0.5 M and an O:A ratio of 2:1as shown in *Figure 15j*. In this case, the minimum co-extraction of Al ∼87% was achieved using a 0.3 M D2EHPA and an O:A ratio of 1:2. When the x_1 (pH) is set to standard level (0=3.2) a slightly lower co-extraction of Al ∼93% was obtained when the concentration of D2EHPA was 0.5 M and the O: A ratio was 2:1, whereas the smallest co-extraction ∼83% was obtained when the D2EHPA concentration was 0.3 M and the O: A ratio was 1:2 in *Figure 15k.* Finally, when x_1 (pH) was adjusted to the lowest level (-1 =2.4), the maximum co-extraction of Al was 60% using 0.5 M D2EHPAand an O: A ratio of 2:1, while the lowest co-extraction was 50% when using 0.3 M D2EHPA and an O: A ratio of 1:2 as shown in *Figure 15l.*

Finally, while discussing surface responses, it is worth noting a few aspects. To begin, at pH 3.33 and 0.42 M D2EHPA, it was possible to achieve Mn extraction efficiencies in the region of 80-90% while maintaining a low co-extraction of Co in the range of 2.5-5% (for the same points). Another noteworthy observation is that when a pH of 3.33 is used in conjunction with 0.5 M D2EHPA, Mn extraction increases to between 90-100%. When the D2EHPA concentration is raised, the co-extraction of Co also rises 7.5-10%. The contour plots representing the extraction efficiencies when varying the pH and concentration of D2EHPA and keeping the O:A ratios constant at each one of the levels can be seen in *Figure S-1* in the Appendix. Additionally, when is examined the interaction between O:A ratios (1.38) and 0.5 M D2EHPA is used, it can be seen another point that results in Mn extraction in the region of 90-100 % and Co extraction in the range of 5-7.5% for pH 3.33. Those points seem to be very compelling. However, additional difficulties, such as co-extraction of Cu and Al, occur and could affect the purity of final products. Therefore, the removal of Cu and Al from the leachate must be optimized by decreasing their concentration in the feed solution (e.g., cementation or precipitation should be done before starting to extract the main metal Mn).

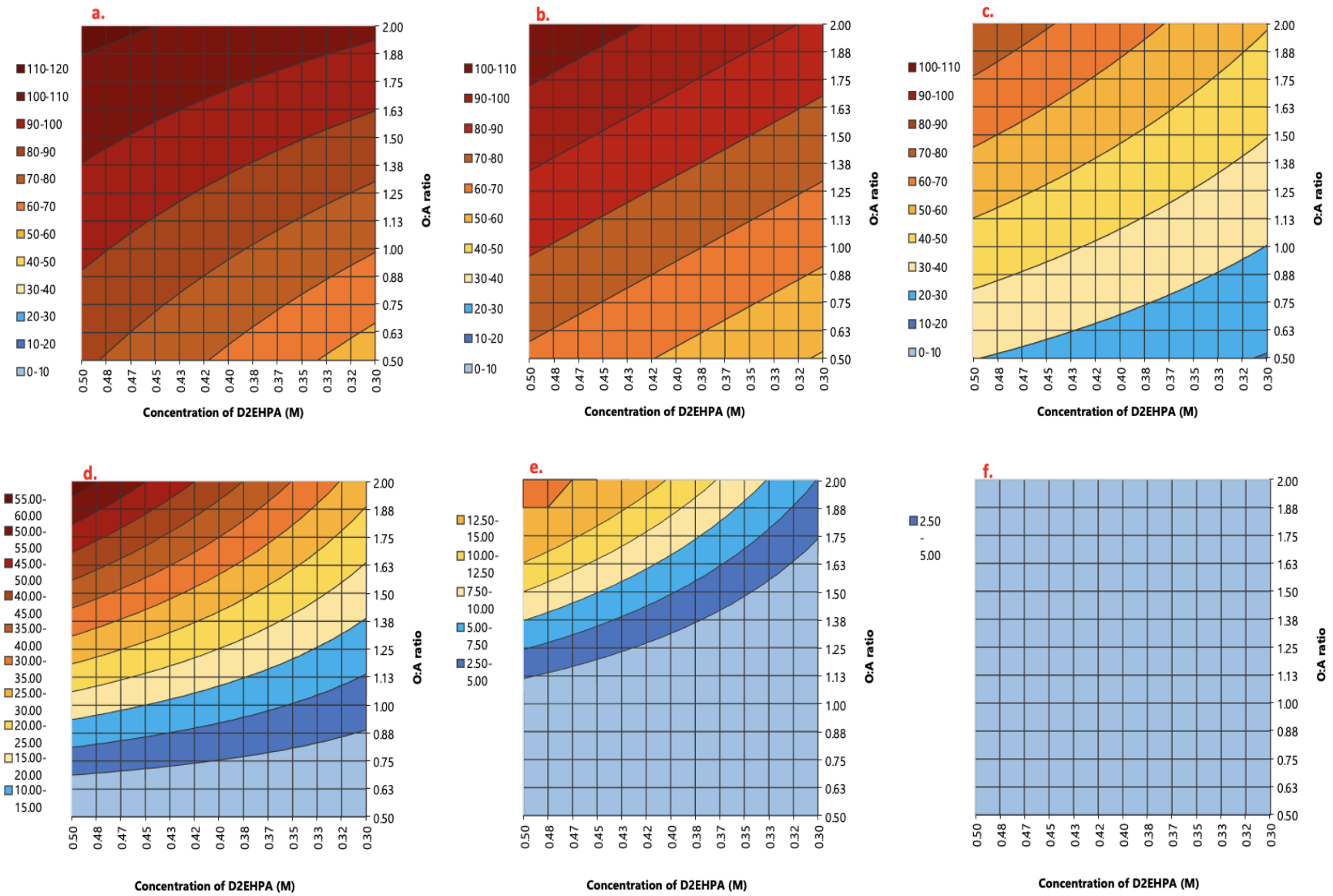
a.
110-120
100-110
90-100
80-90
70-80
60-70
50-60
40-50
30-40
20-30
10-20
0-10
0.50 0.48 0.47 0.45 0.43 0.42 0.40 0.38 0.37 0.35 0.33 0.32 0.30
Concentration of D2EHPA (M)
2.00 1.88 1.75 1.63 1.50 1.38 1.25 1.13 1.00 0.88 0.75 0.63 0.50
O:A ratio
b.
100-110
90-100
80-90
70-80
60-70
50-60
40-50
30-40
20-30
10-20
0-10
0.50 0.48 0.47 0.45 0.43 0.42 0.40 0.38 0.37 0.35 0.33 0.32 0.30
Concentration of D2EHPA (M)
2.00 1.88 1.75 1.63 1.50 1.38 1.25 1.13 1.00 0.88 0.75 0.63 0.50
O:A ratio
c.
100-110
90-100
80-90
70-80
60-70
50-60
40-50
30-40
20-30
10-20
0-10
0.50 0.48 0.47 0.45 0.43 0.42 0.40 0.38 0.37 0.35 0.33 0.32 0.30
Concentration of D2EHPA (M)
2.00 1.88 1.75 1.63 1.50 1.38 1.25 1.13 1.00 0.88 0.75 0.63 0.50
O:A ratio
d.
55.00-60.00
50.00-55.00
45.00-50.00
40.00-45.00
35.00-40.00
30.00-35.00
25.00-30.00
20.00-25.00
15.00-20.00
10.00-15.00
0.50 0.48 0.47 0.45 0.43 0.42 0.40 0.38 0.37 0.35 0.33 0.32 0.30
Concentration of D2EHPA (M)
2.00 1.88 1.75 1.63 1.50 1.38 1.25 1.13 1.00 0.88 0.75 0.63 0.50
O:A ratio
e.
12.50-15.00
10.00-12.50
7.50-10.00
5.00-7.50
2.50-5.00
0.50 0.48 0.47 0.45 0.43 0.42 0.40 0.38 0.37 0.35 0.33 0.32 0.30
Concentration of D2EHPA (M)
2.00 1.88 1.75 1.63 1.50 1.38 1.25 1.13 1.00 0.88 0.75 0.63 0.50
O:A ratio
f.
2.50-5.00
0.50 0.48 0.47 0.45 0.43 0.42 0.40 0.38 0.37 0.35 0.33 0.32 0.30
Concentration of D2EHPA (M)
2.00 1.88 1.75 1.63 1.50 1.38 1.25 1.13 1.00 0.88 0.75 0.63 0.50
O:A ratio

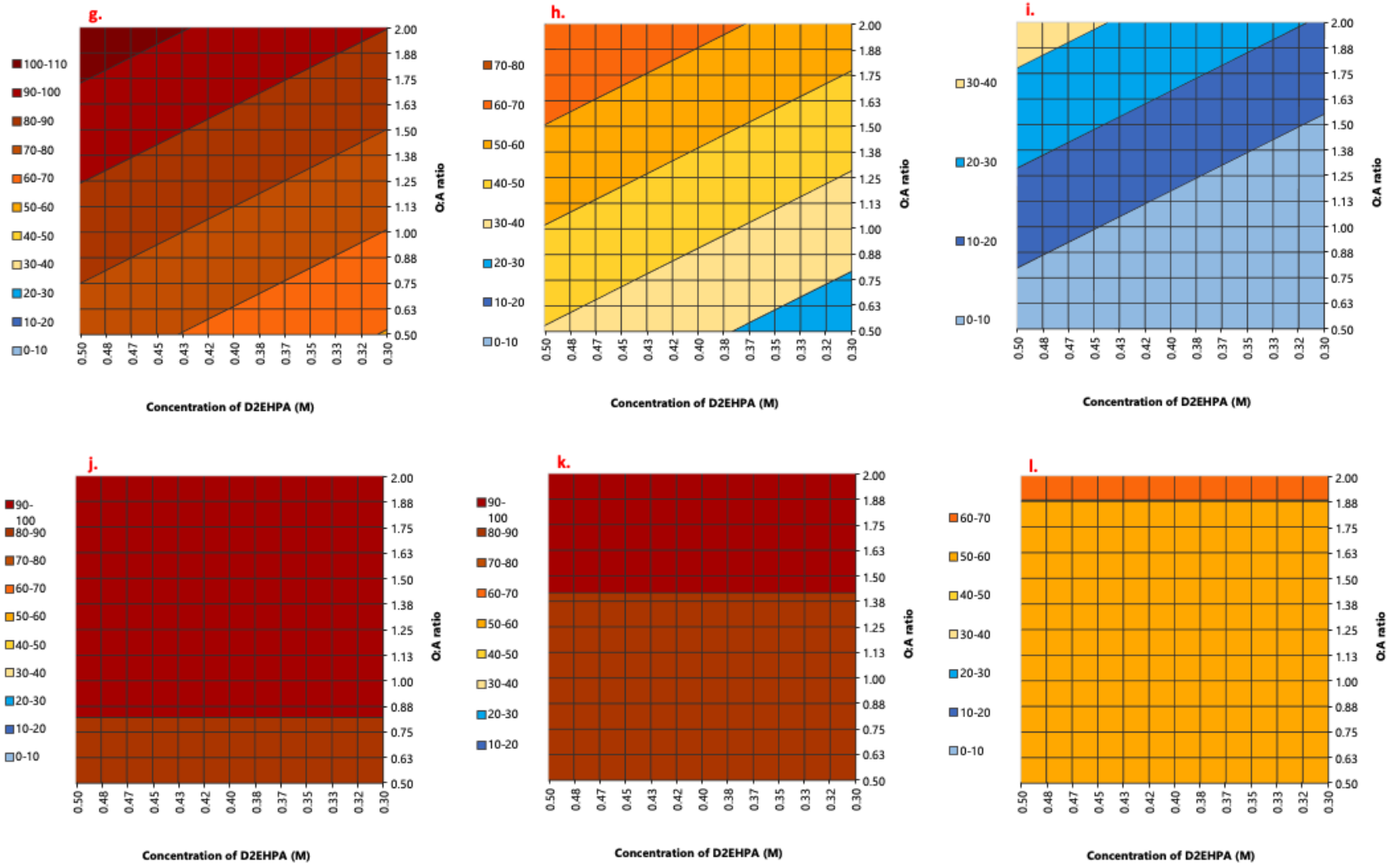

Figure 15.Contour plots depicting the association between different factors in the extraction efficiency of different metals varying the concentration of D2EHPA and O:A ratio (a–c) Mn extraction, co-extraction of (d–f) Co, (g-i) Cu and (j–l) Al at constant pH 4 (a,d,g,j), pH 3.2 (b,e,h,k), and pH 2.4 (c,f,i,l).

After determining the optimal conditions for the extraction operation, the removal of co-extracted impurity metals was investigated during the scrubbing operation. The larger volume of loaded organic was obtained in 1 stage under those conditions to be used in the scrubbing tests. A total of 630 mL of leachate is contained and the equivalent amount of D2EHPA 0.5 M should be applied. Since the O:A ratio is (1:1). Following that, NaOH 10 M was added to adjust the equilibrium pH. Since early experiments suggested that the ideal pH range for extracting Mn while minimizing co-extraction of Co is 3.1-3.2. Thus, 9 mL of NaOH was used in total to achieve the pH range of 3.17.

6.2 Scrubbing operation

Scrubbing is one of the ways being investigated for eliminating unwanted co-extracted metal ion contaminants (e.g., Cu, Al) from the loaded organic. For example, in the case of Mn extraction, a solution containing manganese ions (e.g., $MnSO_4.H_2O$) will be used to substitute metal cations of the co-extracted ion metals by Mn.

6.2.1 Effect of contact time and scrubbing solution on scrubbing efficiency

Scrubbing conditions include maintaining the same O:A ratio (3:1 – 2.25:0.75 ml), using scrubbing solutions containing different concentrations of Mn (2, 4, and 6 g/ L Mn) made of $MnSO_4.H_2O$, and varying the time in the range of 2, 5, 10, 15, and 20 min. The pH of the $MnSO_4.H_2O$ was determined before starting the scrubbing experiments, and it was 4.2, 4.0, and 3.9 for the scrubbing solutions containing 2, 4, and 6 g/L Mn, respectively. The efficiency of the operation was also determined by monitoring the metal concentrations in each phase and using mass balance.

While comparing the three curves of scrubbing solutions 2, 4, and 6 g/L Mn in *Figure 16(a-c)*, it can be seen that for all metals (Co, Li, and Ni), the scrubbing efficiency follows the same trend and increases with time. Among all scrubbing solutions, the one containing 6 g/L Mn led to higher scrubbing efficiencies when compared to scrubbing solutions 2 and 4 g/L Mn. Therefore, the optimal circumstances for continuing development were to perform the following tests using a contact time of 20 min and a scrubbing solution containing 6 g/L Mn. The scrubbing efficiency for Mn was not included in the graphs since the use of a scrubbing solution containing manganese ions ($MnSO_4.H_2O$) lead to an enrichment of Mn in the loaded organic and consequence the efficiencies above 100 %. The standard deviations correspond to triplicates.

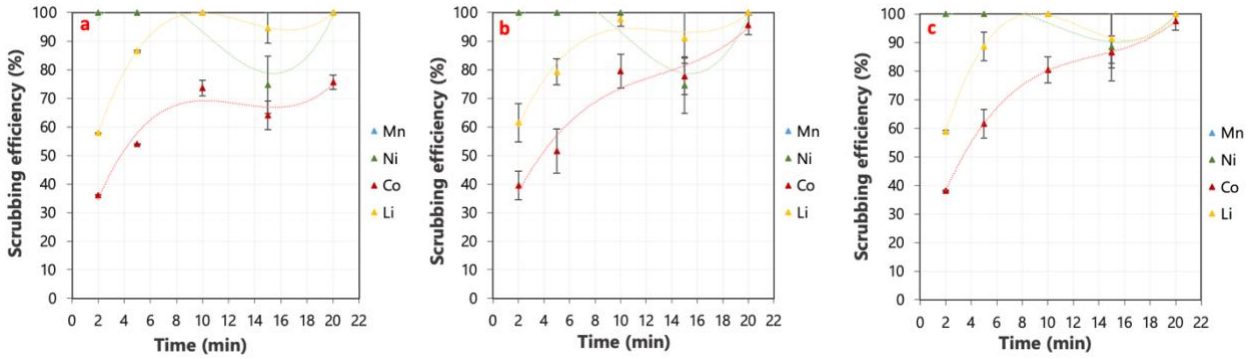

Figure 16. The scrubbing efficiencies of metals (Mn, Ni, Co, and Li) concerning contact time and various scrubbing solutions of 2, 4, and 6 g/L Mn made of $MnSO_4.H_2O$. The experimental conditions are as follows: O:A ratio is 3:1; contact time is varied between 2, 5,10,15, and 20 min.

When comparing the three curves of scrubbing solutions 2, 4, and 6 g/L Mn in *Figure 17(a-c)*, it can be seen that almost all metals (Cu and Mg) exhibit the same trend as in *Figure 16(a-c)*, i.e. scrubbing efficiencies increases with time and that the 6 g/L scrubbing solution has the highest scrubbing efficiency when compared to the 2 and 4 g/L Mn. However, the scrubbing efficiency of Zn and Al is extremely low. The scrubbing efficiency for Zn varies between 0.1-1% for all scrubbing solutions, while the efficiency for Al is constant at 0.4 % regardless of the concentration of the scrubbing solution at 2, 4, and 6 g/L Mn. All trials were conducted in triplicate to ensure test accuracy.

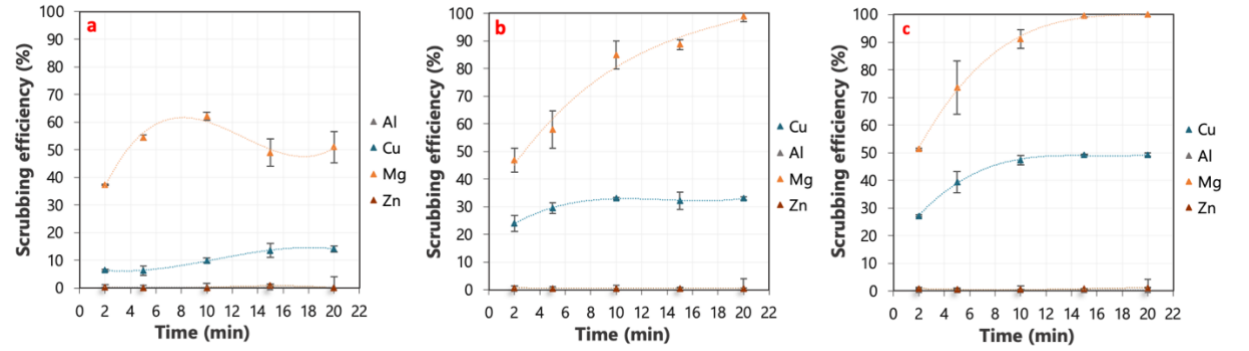

Figure 17. Various scrubbing solutions of (a) 2,(b) 4, and (c) 6 g/L Mn made of $MnSO_4.H_2O$ with experimental conditions for (Cu, Al, Mg, and Zn) metals are as follows: O:A ratio is 3:1; contact time is varied between 2, 5,10,15, and 20 min.

6.2.2 Effect of using water (Milli Q-water) as a scrubbing agent

A preliminary test was performed to investigate the possibility of using water (Milli Q-water) as a scrubbing agent. This test was carried out using an O:A ratio of 3:1 and a contact time of 20 min. The scrubbing efficiency of the different metals is shown in *Figure 18.* Scrubbing is not dependent on water. As can be observed, Milli Q-water has a net low effect on the scrubbing efficiency for the major contaminant metals, which is mostly due to the high hydration and lack of ion-pair formation. [43]The scrubbing efficiency using water was limited. However, Mg, Zn, Li, and Fe corresponded to 32, 24, 19, and 11 %, respectively. But it is known that the concentrations of these metals in the loaded organics are low. Therefore, considering that the primary focus of

this operation is removing co-extracted metals that are present in higher concentrations in the loaded organic, such as Co, Cu, and Al, further tests using Milli Q-water were not attempted.

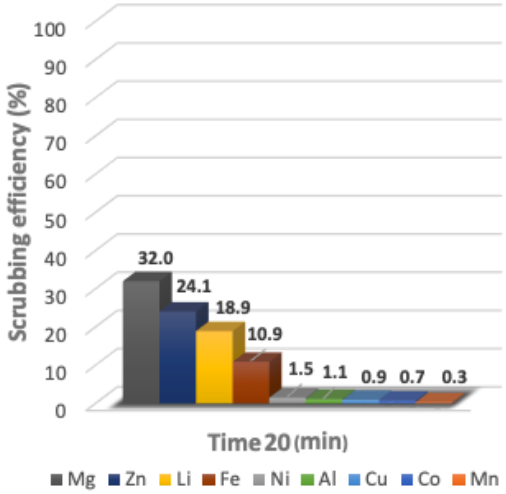

Figure 18. (Milli Q-water) as a scrubbing agent. The experimental conditions are as follows: O:A ratio is 3:1 and contact time is 20 min.

6.2.3 Effect of direct stripping of the loaded organic phase

It employed the direct stripping of the loaded organic phase (by skipping the scrubbing stage). It was tested using different concentrations of sulphuric acid, (H_2SO_4) at 0.1, 0.25, 0.5, 1, 1.5, and 2 M . The O:A ratio was set at 3:1 and the contact time at 15 min and the results can be observed in *Figure 19(a-b).* Regardless of the stripping solution used, the stripping efficiency for Mn and Li is 100%. Co stripping also reaches high efficiencies ~80% regardless of the concentration of the stripping solution. Following that, in *Figure 19b*, can be seen the same trend for the metals Cu, Mg, and Zn, which are also mainly stripped along with Mn. Al is in the (0.9-5) % range, hence it is not much affected by the stripping concentration solution. Fe concentrations are in general below the limit of detection (LOD). As a result, it is possible to conclude that the scrubbing stage is required. If it is omitted, as happened in these trials, it suggests that co-extracted impurities are stripped along with Mn, which could affect the purity of the final Mn product.

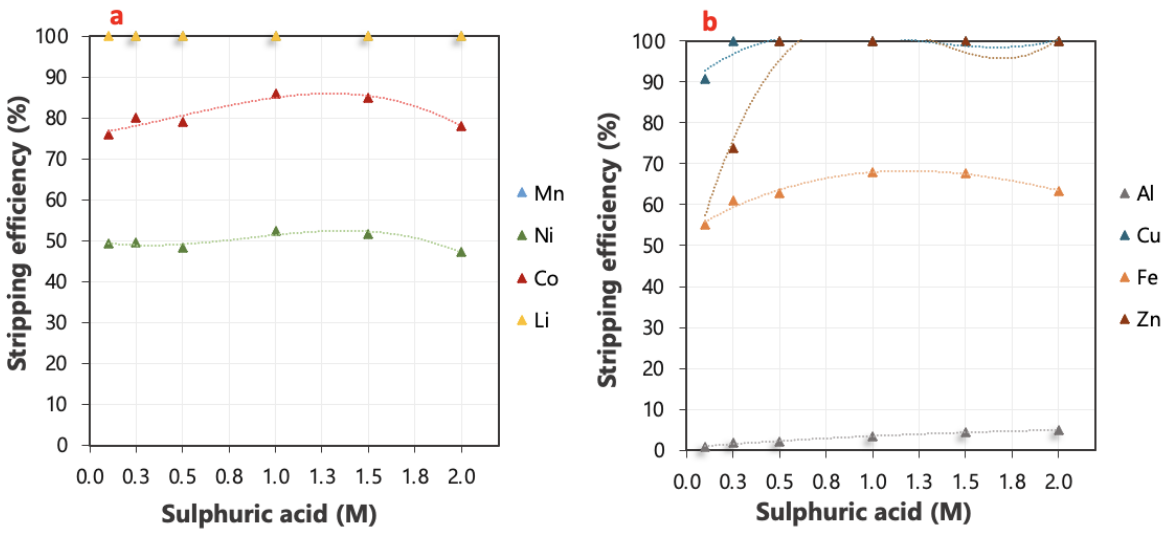

Figure 19. Direct stripping of the loaded organic phase by skipping the scrubbing stage. The experiment's conditions are as follows: O:A ratio is 3:1, the contact time is 15 min, and the sulphuric acid content in the aqueous solution is adjusted between 0.1, 0.25, 0.5, 1, 1.5, and 2 M.

6.2.4 Effect of different ratios O:A with 6 g/L Mn and 20 min

Based on the results from previous tests, it was determined that the contact time for the scrubbing operation ought to be 20 min and the scrubbing solution should have a concentration of 6g/L Mn. Additional experiments were performed to investigate the effect of the O:A ratio on the scrubbing efficiency. The following ratios were tested 3:1, 2.5:1, 2:1, 1.5:1 and 1:1. Co and Li had similar behavior, as can be observed in *Figure 20a.* The fraction of Ni scrubbed remains nearly constant regardless of the O:A ratios. Mn scrubbing efficiency was above 100%, as expected considering the use of a scrubbing solution containing 6 g/L Mn. As the O:A ratio decreases, the scrubbing efficiency increases. The same trend is visible in *Figure 20b* for Cu. However, the effect of changing the O:A ratio is negligible for Zn and Al, with efficiencies of ~1-3 % for Zn and 0.2-4% for Al. Additionally, the scrubbing efficiency of Mg is constant across all O:A ratios. As a result, it is possible to conclude, that the ideal O:A ratio for the scrubbing operation was determined as 1:1. Besides, all trials were conducted in triplicates to ensure experiment accuracy.

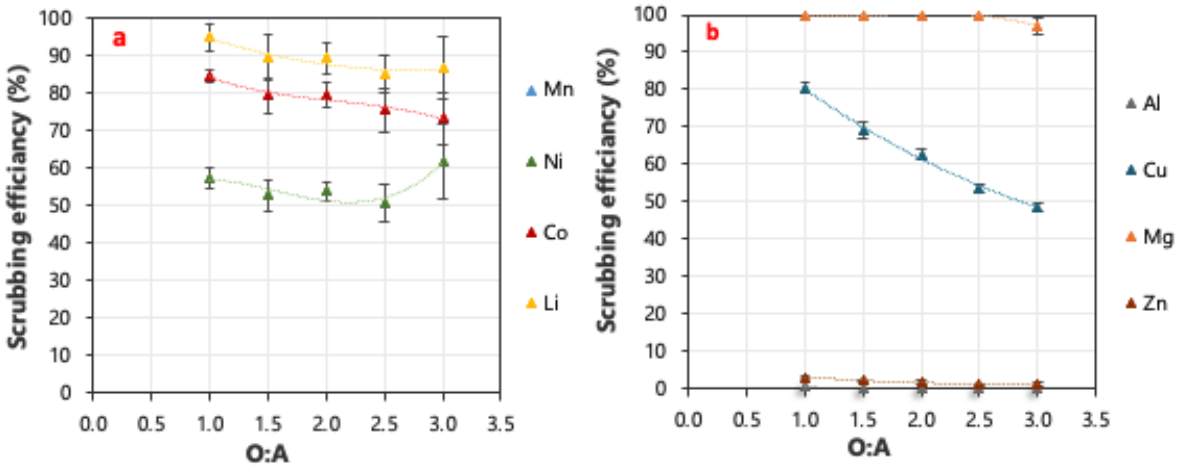

Figure 20. The effect of the O:A ratio on the scrubbing efficiency. The following conditions apply to the experiment: The O:A ratio is set to a value between (3:1, 2.5:1, 2:1, 1.5:1, and 1:1), a contact time of 20 min, and a scrubbing solution ($MnSO_4.H_2O$) concentration of 6 (g/L).

The McCabe-Thiele diagram can be used to calculate the theoretical number of countercurrent scrubbing stages required to efficiently scrub a certain co-extracted metal. In this case, McCabe-Thiele diagrams were constructed representing the scrubbing of Co and Cu from the loaded organic using different O:A ratios of 2:1 and 1:1. The distribution of Co and Cu in the aqueous and organic phases may be observed in *Figure 21(a-d). Figure 21(a,d)* shows that scrubbing of Co and Cu can be accomplished after three and two scrubbing stages with an O:A ratio of 2:1. However, scrubbing in two stages for Cu and Co is optimal for O:A ratios of 1:1 as mentioned above (operation line represented in orange), as illustrated in *Figure 21 (b,c).* The error bars indicate the standard deviation of triplicates measurement.

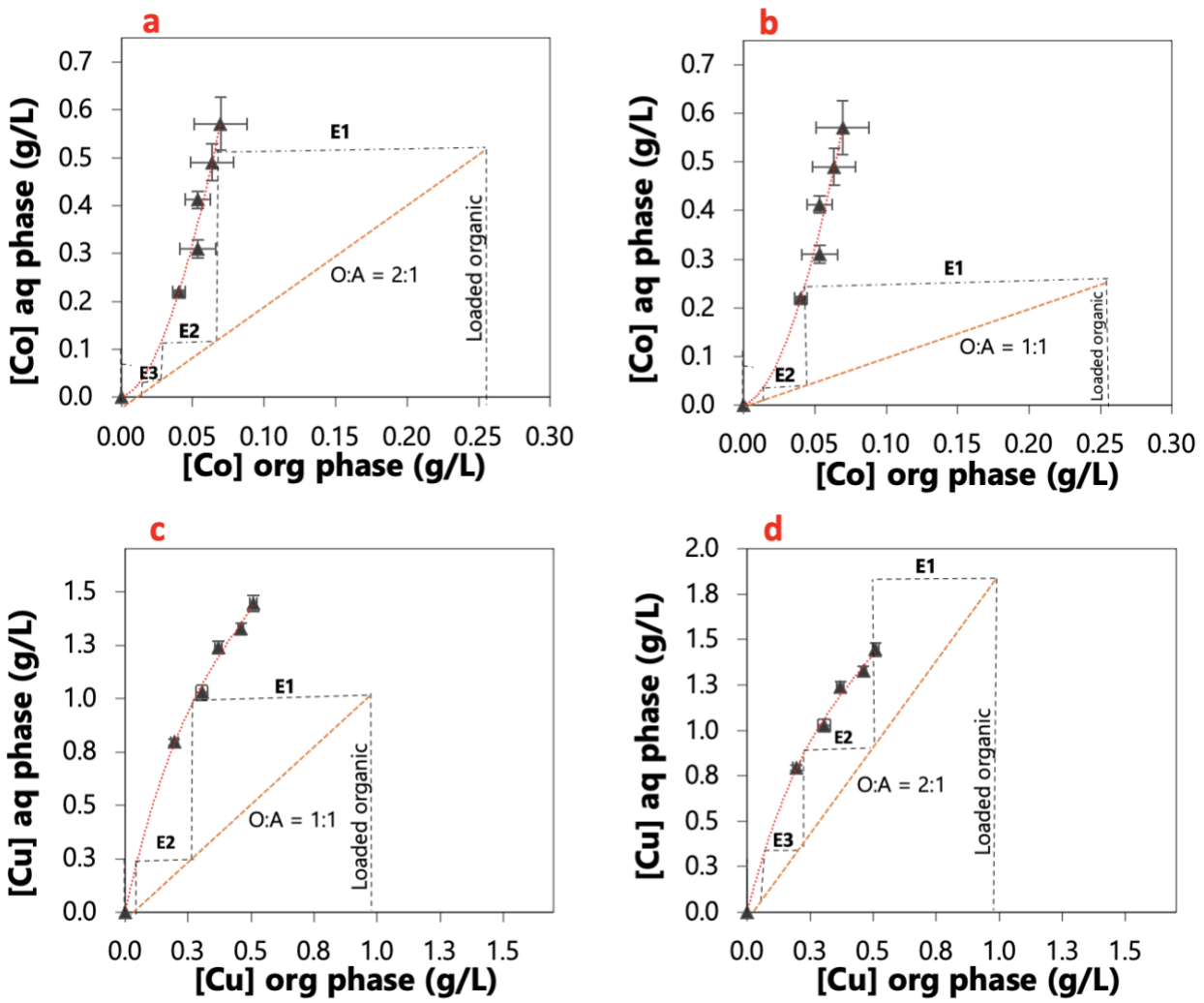

Figure 21. McCabe-Thiele diagram depicting the scrubbing of Co and Cu metals, using different O:A ratios (2:1 and 1:1). Conditions: The O:A ratio is set between (3:1, 2.5:1, 2:1, 1.5:1, and 1:1), the contact time is set to 20 min, and the scrubbing solution ($MnSO4.H_2O$) concentration is set to 6 (g/L).

After determining the optimal conditions for the scrubbing operation. The larger volume of scrubbed loaded organic solution for the stripping stage was prepared based on the optimal scrubbing conditions (e.g., O:A ratio of - 1:1, contact time of 20 min, and 6 g/L of Mn scrubbing solution) in two stages. *Figure 21(a-d)* depicts a McCabe-Thiele diagram of the scrubbing of Co^{2+} and Cu^{2+} metals. In the 1st stage, a total of 150 ml of the organic load is applied together with an equivalent amount of scrubbing solution (6g/L Mn). Considering that the O:A ratio is (1:1). In the 2nd stage, 130 ml of a loaded organic solution is applied (what is left after the 1st stage of the stripping stage). O:A ratio (1:1) remains the same.

6.3 Stripping operation

The goal of the stripping operation is to remove the desired metal ion (i.e., Mn) into the aqueous phase while retaining other high concentration contaminant metals (i.e., Co, Cu, and Al) in the stripped loaded organics.

6.3.1 *Effect of different concentrations of H_2SO_4 acid on the stripping efficiency*

For this goal, stripping tests were conducted to determine the effect of the concentration of H_2SO_4 on stripping efficiency. The H_2SO_4 acid concentration varied in the range of 0.1, 0.25, 0.5, 1, 1.5, and 2 M, the contact time was maintained constant at 15 min, and the O:A ratio was 1:1 using vials of a total volume of 3 ml.

Figure 22 depicts the results of three metals (e.g., Mn, Al, and Zn) with various H_2SO_4 acid concentrations of 0.1, 0.25, 0.5, 1, 1.5, and 2 M. Co, Li, Ni, Fe, Zn, and Mg concentrations were lower than the limit of detection and it was assumed that the stripping efficiency of these metals was 100 %, regardless of H_2SO_4 acid concentration. Using a concentration of 0.1 M H_2SO_4, Zn is stripped with an efficiency of 33%. For the remainder concentration, it reached 100%. Regarding Al, the stripping efficiency ranges between 4-5 %. Thus, the high purity of the final product will be maintained. Since the majority of metals were removed regardless of H_2SO_4 acid concentration, this statement is true. (i.e., Co, Ni, Li, Fe, Zn, and Mg). Therefore, the H_2SO_4 acid concentration was selected based on the Mn stripping efficiency. The most effective stripping concentration was using 0.5 M H_2SO_4 acid as seen in *Figure 22*. In addition, based on the extraction mechanism described in *Equation 4*, a minimum of 0.15 M of extractant per 0.075 M of Mn in loaded organics is required to reverse the reaction. It was possible to select a 0.25 M stripping solution. However, the Mn stripping efficiency of this stripping solution was lower. Therefore, it was agreed to continue experiments with 0.5 M H_2SO_4 in the next investigations. The error bars indicate the standard deviation of triplicates measurement.

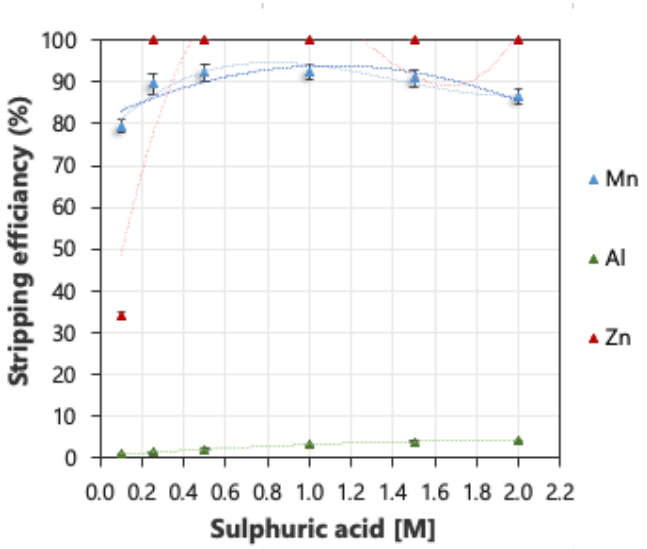

Figure 22. Stripping of the loaded organic phase for metals (Mn, Zn, Al). The experiment's conditions are as follows: O:A ratio is (1:1), the contact time is 15 min, and the H_2SO_4 concentration in the aqueous solution is adjusted between 0.1, 0.25, 0.5, 1, 1.5, and 2 (M).

6.3.2 *Effect of different O:A ratios on the stripping efficiency*

Based on the results of previous tests, it was determined that the stripping solution should include 0.5 M H_2SO_4, and the contact time should continue at 15 minutes. Consequently, additional tests were done to investigate the impact of the O:A ratio on the stripping efficiency. These ratios were evaluated: 3:2, 2.5:1, 2:1, 1.5:1, 1:1, and 1:1.5. The objective is to maintain a low concentration of the aqueous solution (H_2SO_4). Since it can be utilized with mixer-settlers or larger volumes (industrial scale). It is undesirable to have an excessive amount of stripping solution (H_2SO_4) as a byproduct. Which must then be neutralized with NaOH. As a result, it will produce a byproduct and take extra steps to neutralize it. Which will be more expensive? Thus, the O:A ratio is crucial, to achieving high stripping efficiency while minimizing H_2SO_4 acid consumption.

Co, Li, Ni, Fe, and Mg concentrations were below the limit of detection, and it was assumed that the stripping efficiency of these metals was 100 %, regardless of O:A ratios (for this reason they are omitted from *Figure 23*). As seen in *Figure 23* for selected metals (Mn, Al, Zn) the reversal outcome is easily identifiable from the extraction stage (when the O:A ratio increases, so do the extraction efficiency). Hence, when the O:A ratio decreases, so does the stripping efficiency. The most efficient stripping O:A ratios for Mn are 1:1 and 1:1.5. As indicated previously, it is preferable to maintain a low concentration of H_2SO_4 acid while achieving a high stripping efficiency. This indicates that O:A - 1:1 meets this criterion the best. The error bars indicate the standard deviation of triplicates measurement.

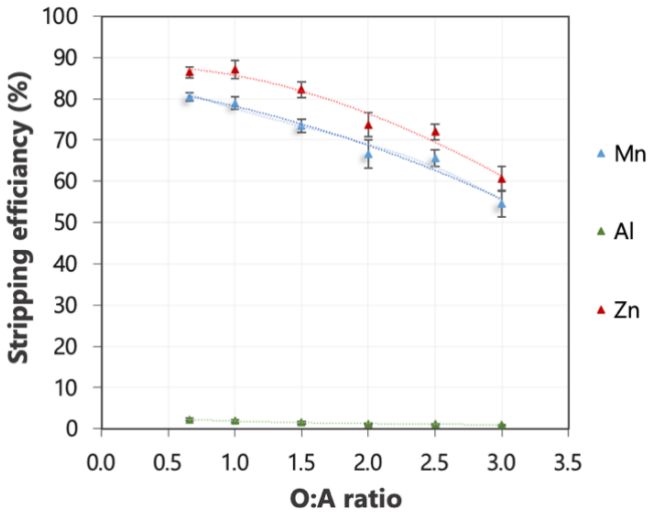

Figure 23. The effect of the O:A ratio on the stripping efficiency. Conditions: contact time of 15 min, and 0.5 M H_2SO_4.

The McCabe-Thiele diagram can be used to calculate the theoretical number of stripping stages required to efficiently strip the targeted metal (i.e., Mn). In this case, a McCabe-Thiele diagram was constructed representing the stripping of Mn from the loaded organic using an operational line of O:A ratio 1:1. The distribution of Mn in the aqueous and organic phases may be observed in *Figure 24*. Based on *Figure 24*, it is possible to conclude that optimal stripping of Mn can be accomplished after three stripping stages with an O:A ratio of 1:1 (operation line represented in orange). Approximately 80 % Mn can be stripped in the first stage, while the

remaining 20 % can be removed in two more stages. The error bars represent the standard deviation (horizontal versus vertical) of measurements made in triplicate.

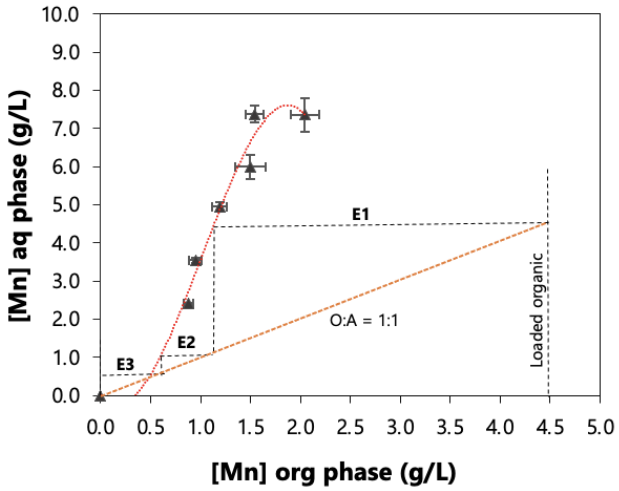

Figure 24. McCabe-Thiele diagram depicting the stripping of Mn concentration in the loaded organic: 4495 mg/L. Conditions: contact time of 15 min using 0.5 M H_2SO_4.

The scrubbing and stripping efficiencies for various metals (Mn, Co, Li, Ni, Cu, Al, Zn, Mg, and Fe) are shown in the final four rows of *Table 5*, which contain two scrubbing stages and one stripping stage of loaded organics.

Table 5 Distribution of metals starting from the extraction stage (initial concentration) until stripping operation. Scr ST1(scrubbing stage 1), Scr ST1 (scrubbing stage 2), StrST1(stripping stage 1), StrST2(stripping stage 2)ST1(stage 1), and ST2 (stage 2)

Stage	***Concentration (mg/L)***								
Metals	*Mn*	*Co*	*Li*	*Ni*	*Cu*	*Al*	*Zn*	*Mg*	*Fe*
Leachate	2055 (100%)	2666 (100%)	908 (100%)	2429	1340 (100%)	340 (100%)	2.35	3.6	10.2
Raffinate	229 (11%)	2523 (94.7%)	887 (97.8%)	2349	466 (35%)	58 (18%)	0.02	2.6	0.8
Loaded organic	1825 (89%)	143 (5.3%)	20 (2.2%)	80	874 (65%)	280 (82%)	2.33	1	9.45
ScrST1 (Raffinate)	3902	192	40	47	687	16	0.09	1.4	11
ScrST2 (Raffinate)	5528	2	5	5	174	15	0.06	0.4	14
ST1 - scrubbed Loaded organic	3973	0 (100%)	0 (100%)	0 (100%)	187 (78%)	266 (5.6%)	2.23 (3.8%)	0 (100%)	0 (100%)
ST2- scrubbed Loaded organic	4495	0 (100%)	0 (100%)	0 (100%)	0 (100%)	250 (11.2%)	2.17(6.4%)	0 (100%)	0 (100%)
StrST1 (Raffinate)	3618	0	0	0	0	10	0	0	0
ST1 - stripped Loaded organic	876 (80%)	0	0	0	0	240 (4%)	0.27 (88%)	0	0

According to *Table 5*, the concentration of Mn in the raffinate rises from Scrubbing Stage 1 (ScrST1) to Scrubbing Stage 2 (ScrST2). Due to the application of 6 g/L of Mn scrubbing solution. The McCabe-Thiele diagram in *Figure 21* demonstrates that Cu can be scrubbed in two stages. In the 1st stage, it reached 78%, and in the 2nd, it was eliminated by 100%. In addition, Al and Zn are still present in loaded organics after two stages of scrubbing operation. For Al in the 1st stage, 3.1% is scrubbed, while in the 2nd stage, only 4.8% is scrubbed. Comparable conditions can be observed with Zn (1st stage 3.8% and 2nd stage 6.4%); however, the concentration in loaded organics is significantly lower than Al content. As a result, the Zn content is relatively low. For anyone interested in this topic to resolve this issue, various extractants or ion exchange could be used. Regarding Al content, it must be handled similarly to how Cu content was addressed. Before starting the extraction process, it must be removed through additional pretreatment (i.e., precipitation). Lastly, a single stripping stage can yield a stripping Mn product containing approximately 3.6 g/L (80%) Mn and ~0.008 g/L (4%) of Al, respectively.

Figure 25 depicts the final process flowchart for extraction, scrubbing, and stripping experiments with all optimal conditions for each stage.

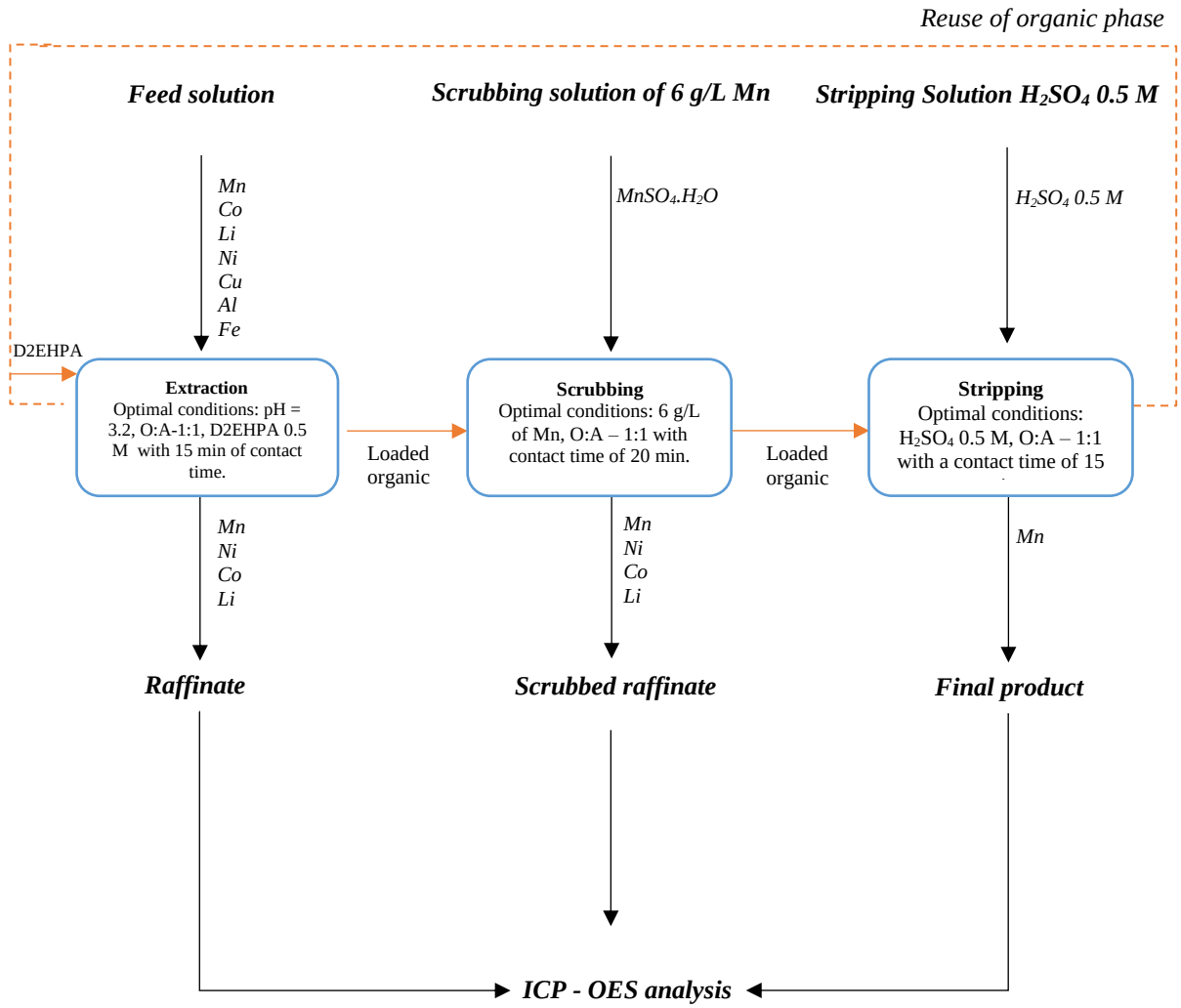

Figure 25. General process flowchart of extraction, scrubbing and stripping for all performed experiments under optimal conditions. Black lines represent the aqueous phase and orange the organic phase.

7. Conclusion

In this master thesis work, the extraction of manganese from leachate solution derived from spent LiBs was examined using solvent extraction. Utilizing techniques such as the factorial design of experiments and response surface methodology, it was possible to investigate the interactions of many critical factors that controlled the maximization of Mn extraction while minimizing the co-extraction of impurity metals (i.e, Co, Cu, and Al). In addition, scrubbing and stripping were also investigated.

Initially, exploratory experiments were conducted to determine the factors that influence the solvent extraction of Mn, and subsequently, the ideal conditions were identified and used in a factorial design of experiments to generate models for the metals of greatest relevance (i.e Mn, Co).

Based on preliminary results, the most relevant parameters, such as the molar concentration of extract D2EHPA, the O:A ratio, and the equilibrium pH, were taken into account. Based on these important factors, the following are the optimal parameters for the extraction phase: 0.5 M D2EHPA, O: A - 1:1, pH: 3.2. Under these conditions, about 89% Mn and 2.5 % Co were extracted in a single stage. However, there is very little co-extraction of Li and Ni. Which is for Li ~1% and Ni (not extracted - 0%). On the other hand, the co-extraction of Cu and Al was high (60% and 94%). The McCabe-Thiele diagram revealed that when using an O:A ratio of 1:1, two extraction stages are required to fully extract Mn.

The presence of co-extracted metals in the loaded organic led to the development of a scrubbing stage, with the primary objective of reducing the concentration of co-extracted metals. Under the circumstances examined for the scrubbing stage, the most important parameters, including the molar concentration of the scrubbing solution, the O:A ratios, and the contact time, were considered. Scrubbing solutions containing manganese in various concentrations were produced, such as 2, 4, and 6 g/L Mn (made from $MnSO_4.H_2O$). Co-extracted metals were scrubbed the most effective when using a 6 g/L Mn. The following are the best parameters for the scrubbing phase based on the consideration of these crucial factors: scrubbing solution containing 6 g/L Mn, an O:A ratio - 1:1, and contact time of - 20 min. According to the McCabe-Thiele diagram, when using an O:A ratio - 1:1, two scrubbing stages are required to efficiently remove the co-extracted Co and Cu.

To recover the desired metal ion (i.e., Mn) from the loaded organic to an acidic solution, the stripping stage was investigated. The factors considered for the improvement of the stripping stage were the H_2SO_4 concentration, the O:A ratio, and the stripping time, which was held constant. Under optimal conditions (O:A ratio of 1:1, 0.5 M H_2SO_4, and contact time of 15 min), a single stripping stage can yield a stripping product containing approximately 3.6 g/L (80%) Mn and ~0.008 g/L of Al, respectively. According to the McCabe-Thiele diagram, Mn can be optimally stripped in three stages with an O:A ratio of 1:1.

Using solvent extraction with D2EHPA followed by scrubbing, and stripping procedures, it is possible to recover Mn from spent lithium-ion batteries, which are a significant secondary source of Mn. The results gained from the utilized procedures are based on well-established unit processes, the created process has a high potential for large-scale applications or can help further research in this area. In addition, the fitted regression model and surface methodology responses can aid in the optimization of the process, given that many combinations of parameters can result in high Mn extraction and low co-extractions of other impurity metals. In addition, it can

contribute to the building of distribution isotherms of McCabe–Thiele diagrams, which are extremely effective in predicting the distribution of metals in both phases of the system and for determining the theoretical number of required stages. All these options can help design a procedure with reduces costs and environmental impacts.

8. Bibliography

[1] W. F. Cannon, "Manganese: it turns iron into steel (and does so much more)," *Fact Sheet*, 2014, doi: 10.3133/FS20143087.

[2] "Researchers eye manganese as key to safer, cheaper lithium-ion batteries | Argonne National Laboratory." https://www.anl.gov/article/researchers-eye-manganese-as-key-to-safer-cheaper-lithiumion-batteries (accessed Mar. 11, 2022).

[3] "Manganese, nickel, silicon are main focus of battery research - MINING.COM." https://www.mining.com/manganese-nickel-silicon-main-focus-of-battery-research/ (accessed Mar. 11, 2022).

[4] K. Zhang, X. Han, Z. Hu, X. Zhang, Z. Tao, and J. Chen, "Nanostructured Mn-based oxides for electrochemical energy storage and conversion," *Chemical Society Reviews*, vol. 44, no. 3, pp. 699–728, Jan. 2015, doi: 10.1039/C4CS00218K.

[5] W. Chen *et al.*, "A manganese–hydrogen battery with potential for grid-scale energy storage," *Nature Energy 2018 3:5*, vol. 3, no. 5, pp. 428–435, Apr. 2018, doi: 10.1038/s41560-018-0147-7.

[6] S. Bi, S. Wang, F. Yue, Z. Tie, and Z. Niu, "A rechargeable aqueous manganese-ion battery based on intercalation chemistry," *Nature Communications 2021 12:1*, vol. 12, no. 1, pp. 1–11, Nov. 2021, doi: 10.1038/s41467-021-27313-5.

[7] P. Díaz-Arista, R. Antaño-López, Y. Meas, … R. O.-E., and undefined 2006, "EQCM study of the electrodeposition of manganese in the presence of ammonium thiocyanate in chloride-based acidic solutions," *Elsevier*, Accessed: Mar. 11, 2022. [Online]. Available: https://www.sciencedirect.com/science/article/pii/S0013468605013988

[8] "• Projected lithium-ion battery market size worldwide | Statista." https://www.statista.com/statistics/1011187/projected-global-lithium-ion-battery-market-size/ (accessed Mar. 11, 2022).

[9] "• Projected global battery demand by application | Statista." https://www.statista.com/statistics/1103218/global-battery-demand-forecast/ (accessed Mar. 11, 2022).

[10] "• Battery minerals global clean energy demand growth index 2040 | Statista." https://www.statista.com/statistics/1270191/demand-growth-index-of-battery-minerals-for-clean-energy-worldwide/ (accessed Mar. 11, 2022).

[11] S. R. Sunil, S. Vishvakarma, A. Barnwal, and N. Dhawan, "Processing of Spent Li-Ion Batteries for Recovery of Cobalt and Lithium Values," *JOM*, vol. 71, no. 12, pp. 4659–4665, Dec. 2019, doi: 10.1007/S11837-019-03540-6/FIGURES/7.

[12] C. Peng, C. Chang, Z. Wang, B. P. Wilson, F. Liu, and M. Lundström, "Recovery of High-Purity MnO2 from the Acid Leaching Solution of Spent Li-Ion Batteries," *JOM*, vol. 72, no. 2, pp. 790–799, Feb. 2020, doi: 10.1007/S11837-019-03785-1/FIGURES/5.

[13] "Manganese Price 2022 [Updated Daily] - Metalary." https://www.metalary.com/manganese-price/ (accessed Mar. 11, 2022).

[14] S. Al-Thyabat, T. Nakamura, E. Shibata, and A. Iizuka, "Adaptation of minerals processing operations for lithium-ion (LiBs) and nickel metal hydride (NiMH) batteries recycling: Critical review," *Minerals Engineering*, vol. 45, pp. 4–17, May 2013, doi: 10.1016/J.MINENG.2012.12.005.

[15] W. Xuan, A. de Souza Braga, and A. Chagnes, "Development of a Novel Solvent Extraction Process to Recover Cobalt, Nickel, Manganese, and Lithium from Cathodic Materials of Spent Lithium-Ion Batteries," *ACS Sustainable Chemistry and Engineering*, vol. 10, no. 1, pp. 582–593, Jan. 2022, doi: 10.1021/ACSSUSCHEMENG.1C07109/ASSET/IMAGES/MEDIUM/SC1C07109_0012.GIF.

[16] J. B. Goodenough, "How we made the Li-ion rechargeable battery," *Nature Electronics 2018 1:3*, vol. 1, no. 3, pp. 204–204, Mar. 2018, doi: 10.1038/s41928-018-0048-6.

[17] C. C. Wang, Y. C. Lin, K. F. Chiu, H. J. Leu, and T. H. Ko, "Advanced Carbon Cloth as Current Collector for Enhanced Electrochemical Performance of Lithium-Rich Layered Oxide Cathodes," *ChemistrySelect*, vol. 2, no. 16, pp. 4419–4427, May 2017, doi: 10.1002/SLCT.201700420.

[18] "The 4 major components of the lithium-ion battery - Blog - Hopax Fine Chemicals." https://www.hopaxfc.com/en/blog/the-4-major-components-of-the-lithium-ion-battery (accessed Mar. 16, 2022).

[19] H. Xu, Z. Sun, and J. Chen, "Graphene-based anode materials for lithium-ion batteries," *Emerging 2D Materials and Devices for the Internet of Things*, pp. 139–164, Jan. 2020, doi: 10.1016/B978-0-12-818386-1.00006-0.
[20] G. Ledung, "State of the art in reuse and recycling of lithium-ion batteries-a research review State-of-the-art in reuse and recycling of lithium-ion batteries-A research review by Hans Eric Melin, Circular Energy Storage".
[21] "Analysis of the major recycling processes in the battery industry | CIC energiGUNE." https://cicenergigune.com/en/blog/major-recycling-processes-battery-industry (accessed Mar. 25, 2022).
[22] G. Harper *et al.*, "Recycling lithium-ion batteries from electric vehicles," *Nature 2019 575:7781*, vol. 575, no. 7781, pp. 75–86, Nov. 2019, doi: 10.1038/s41586-019-1682-5.
[23] S. Kim *et al.*, "A comprehensive review on the pretreatment process in lithium-ion battery recycling," *Journal of Cleaner Production*, vol. 294, p. 126329, Apr. 2021, doi: 10.1016/J.JCLEPRO.2021.126329.
[24] J. Xiao, J. Guo, L. Zhan, and Z. Xu, "A cleaner approach to the discharge process of spent lithium ion batteries in different solutions," *Journal of Cleaner Production*, vol. 255, p. 120064, May 2020, doi: 10.1016/J.JCLEPRO.2020.120064.
[25] J. Li, G. Wang, Z. X.-W. Management, and undefined 2016, "Generation and detection of metal ions and volatile organic compounds (VOCs) emissions from the pretreatment processes for recycling spent lithium-ion batteries," *Elsevier*, Accessed: Apr. 19, 2022. [Online]. Available: https://www.sciencedirect.com/science/article/pii/S0956053X16300976
[26] T. Zhang, Y. He, L. Ge, R. Fu, X. Zhang, and Y. Huang, "Characteristics of wet and dry crushing methods in the recycling process of spent lithium-ion batteries," *Journal of Power Sources*, vol. 240, pp. 766–771, Oct. 2013, doi: 10.1016/J.JPOWSOUR.2013.05.009.
[27] T. Tran and V. T. Luong, "Lithium Production Processes," *Lithium Process Chemistry: Resources, Extraction, Batteries, and Recycling*, pp. 81–124, Jan. 2015, doi: 10.1016/B978-0-12-801417-2.00003-7.
[28] C. K. Lee and K. I. Rhee, "Preparation of LiCoO2 from spent lithium-ion batteries," *Journal of Power Sources*, vol. 109, no. 1, pp. 17–21, Jun. 2002, doi: 10.1016/S0378-7753(02)00037-X.
[29] W. Lv, Z. Wang, H. Cao, Y. Sun, Y. Zhang, and Z. Sun, "A Critical Review and Analysis on the Recycling of Spent Lithium-Ion Batteries," *ACS Sustainable Chemistry and Engineering*, vol. 6, no. 2, pp. 1504–1521, Feb. 2018, doi: 10.1021/ACSSUSCHEMENG.7B03811/ASSET/IMAGES/LARGE/SC-2017-03811A_0006.JPEG.
[30] J. C. Y. Jung, P. C. Sui, and J. Zhang, "A review of recycling spent lithium-ion battery cathode materials using hydrometallurgical treatments," *Journal of Energy Storage*, vol. 35, p. 102217, Mar. 2021, doi: 10.1016/J.EST.2020.102217.
[31] P. B. Warey, "New research on hazardous materials," p. 421, 2007.
[32] A. Rahman and R. Afroz, "Lithium battery recycling management and policy," *International Journal of Energy Technology and Policy*, vol. 13, no. 3, pp. 278–291, 2017, doi: 10.1504/IJETP.2017.084497.
[33] V. S. Kislik, "Solvent Extraction," *Solvent Extraction*, 2012, doi: 10.1016/C2010-0-65805-6.
[34] Yamina Boukraa, "Extraction of Cobalt and Lithium from Sulfate Solution Using Di(2-ethylhexyl)phosphoric Acid/Kerosene Mixed Extractant," *Russian Journal of Physical Chemistry A*, vol. 94, no. 6, pp. 1136–1142, Jun. 2020, doi: 10.1134/S0036024420060321/FIGURES/6.
[35] "Bis(2-ethylhexyl) phosphate | SIELC." https://www.sielc.com/bis2-ethylhexyl-phosphate.html (accessed May 22, 2022).
[36] J. Stefaniak, S. Karwacka, M. Janiszewska, A. Dutta, E. R. Rene, and M. Regel-Rosocka, "Co(II) and Ni(II) transport from model and real sulfate solutions by extraction with bis(2,4,4-trimethylpentyl)phosphinic acid (Cyanex 272)," *Chemosphere*, vol. 254, p. 126869, Sep. 2020, doi: 10.1016/J.CHEMOSPHERE.2020.126869.
[37] V. T. Nguyen, J. C. Lee, J. Jeong, B. S. Kim, and B. D. Pandey, "The separation and recovery of nickel and lithium from the sulfate leach liquor of spent lithium ion batteries using PC-88A," *Korean Chemical Engineering Research*, vol. 53, no. 2, pp. 137–144, Apr. 2015, doi: 10.9713/KCER.2015.53.2.137.
[38] J.-W. Ahn, H.-J. Ahn, S.-H. Son, and K.-W. Lee, "Solvent Extraction of Ni and Li from Sulfate Leach Liquor of the Cathode Active Materials of Spent Li-ion Batteries by PC88A," *Resources Recycling*, vol. 21, no. 6, pp. 58–64, Dec. 2012, doi: 10.7844/KIRR.2012.21.6.58.
[39] X. Chen and T. Zhou, "Hydrometallurgical process for the recovery of metal values from spent lithium-ion batteries in citric acid media," *Waste Management and Research*, vol. 32, no. 11, pp. 1083–1093, Nov. 2014, doi: 10.1177/0734242X14557380.

[40] M. R. Hossain, S. Nash, G. Rose, and S. Alam, “Cobalt loaded D2EHPA for selective separation of manganese from cobalt electrolyte solution,” *Hydrometallurgy*, vol. 107, no. 3–4, pp. 137–140, May 2011, doi: 10.1016/J.HYDROMET.2011.02.011.

[41] D. C. Montgomery and J. Wiley, “D esign and Analysis of Experiments Eighth Edition,” 2013, Accessed: Apr. 30, 2022. [Online]. Available: www.wiley.com/go/permissions.

[42] “CSIRO Research Publications Repository - Manganese metallurgy review. Part 1: Leaching of ores/secondary materials and recovery of electrolytic/chemical manganese dioxide.” https://publications.csiro.au/rpr/pub?list=BRO&pid=procite:674f5463-e645-4e75-9a42-0c0ac67b0cdc (accessed May 02, 2022).

[43] B. Dewulf, S. Riaño, and K. Binnemans, “Separation of heavy rare-earth elements by non-aqueous solvent extraction: Flowsheet development and mixer-settler tests,” *Separation and Purification Technology*, vol. 290, p. 120882, Jun. 2022, doi: 10.1016/J.SEPPUR.2022.120882.

Appendix

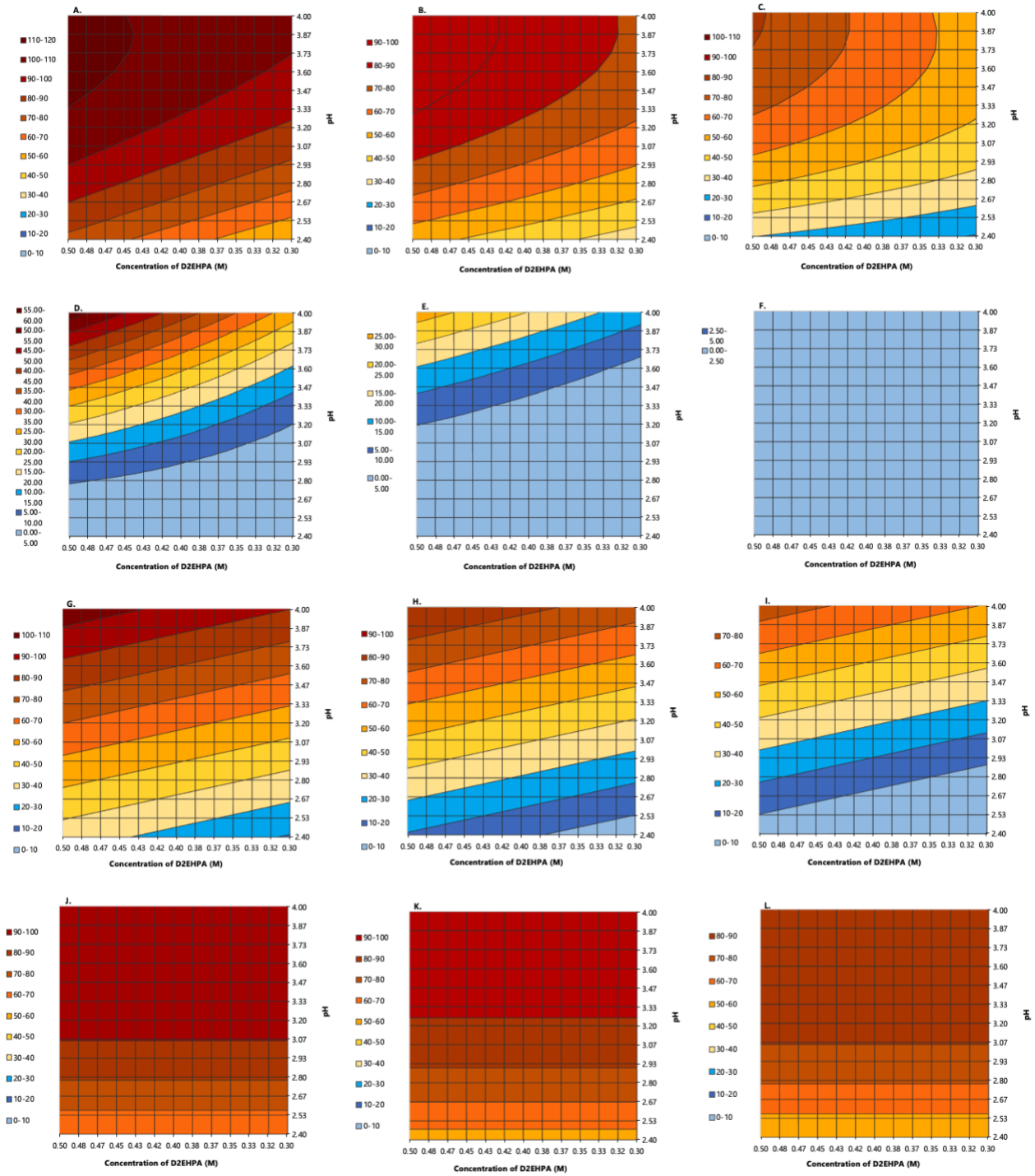

Figure S-1. Contour plots depicting manganese extraction based on concentration of D2EHPA & pH (a–c), coextraction of cobalt (d–f), coextraction of copper (g-i), and coextraction of aluminum (j–l) at pH 4 (a,d,g,j), pH 3.2 (b,e,h,k), and pH 2.4 (j–l) (c,f,i,l).